



Arsenic Water Technology Partnership

Arsenic Removal by Iron-Modified Activated Carbon



About the Water Research Foundation

The Water Research Foundation is a member-supported, international, nonprofit organization that sponsors research to enable water utilities, public health agencies, and other professionals to provide safe and affordable drinking water to consumers.

The Foundation's mission is to advance the science of water to improve the quality of life. To achieve this mission, the Foundation sponsors studies on all aspects of drinking water, including supply and resources, treatment, monitoring and analysis, distribution, management, and health effects. Funding for research is provided primarily by subscription payments from approximately 1,000 utilities, consulting firms, and manufacturers in North America and abroad. Additional funding comes from collaborative partnerships with other national and international organizations, allowing for resources to be leveraged, expertise to be shared, and broad-based knowledge to be developed and disseminated. Government funding serves as a third source of research dollars.

From its headquarters in Denver, Colorado, the Foundation's staff directs and supports the efforts of more than 800 volunteers who serve on the board of trustees and various committees. These volunteers represent many facets of the water industry, and contribute their expertise to select and monitor research studies that benefit the entire drinking water community.

The results of research are disseminated through a number of channels, including reports, the Web site, conferences, and periodicals.

For subscribers, the Foundation serves as a cooperative program in which water suppliers unite to pool their resources. By applying Foundation research findings, these water suppliers can save substantial costs and stay on the leading edge of drinking water science and technology. Since its inception, the Foundation has supplied the water community with more than \$300 million in applied research.

More information about the Foundation and how to become a subscriber is available on the Web at **www.WaterRF.org**.

Arsenic Removal by Iron-Modified Activated Carbon

Prepared by:

Min Jang, Weifang Chen, Jiying Zou, Fred S. Cannon, and Brian A. Dempsey

The Pennsylvania State University

Department of Civil and Environmental Engineering

212 Sackett Engineering Building

University Park, PA 16802

Jointly Sponsored by:

Water Research Foundation

6666 West Quincy Avenue, Denver CO 80235-3098

and

U.S. Department of Energy

Washington, D.C. 20585-1290

Published by:

WERC, a Consortium for
Environmental Education and
Technology Development at
New Mexico State University



Water Research Foundation



DISCLAIMER

This study was jointly funded by the Water Research Foundation and Sandia National Laboratories (SNL) under Agreement No. FI061030711 through the Arsenic Water Technology Partnership. The comments and views detailed herein may not necessarily reflect the views of the Water Research Foundation, its officers, directors, affiliates or agents, or the views of SNL and the Arsenic Water Technology Partnership. The mention of trade names for commercial products does not represent or imply the approval or endorsement of Water Research Foundation or SNL. This report is presented solely for informational purposes.

Copyright © 2010
by Water Research Foundation and Arsenic Water Technology Partnership

ALL RIGHTS RESERVED.
No part of this publication may be copied, reproduced
or otherwise utilized without permission.

Printed in the U.S.A.

CONTENTS

TABLES	VII
FIGURES	IX
FOREWORD	XI
ACKNOWLEDGMENTS	XIII
EXECUTIVE SUMMARY	XV
CHAPTER 1 INTRODUCTION	1
Background	1
Chemistry of Arsenic	1
Arsenic Immobilization	1
Speciation.....	2
Arsenic Adsorption Technologies.....	3
Hydrous Ferric Oxide (HFO) Incorporated Granular Activated Carbon.....	4
Effect of Citrate Ion Addition on Iron Precursors	5
Effect Of Temperature on Preparation of Iron Modified GAC	5
Cationic Surfactant Loaded Onto Fe-Incorporated Gac	6
Objectives	6
Prior and Parallel Research at Penn State	7
Column Tests Using Rutland Groundwater.....	7
Sequential Incipient Wetness Impregnation of Ferrous onto Fe-GAC.....	8
Cationic Surfactant Loaded onto Fe-incorporated GAC	9
Kinetic Studies	9
CHAPTER 2 MATERIALS AND METHODS	17
Materials	17
Activated Carbons.....	17
Water Source.....	17
Chemicals.....	17
Analytical Protocols.....	17
Arsenic Analysis	17
Iron Analysis	18
X-ray Diffraction Analysis	18
Methods.....	18
Rapid Small-scale Column Tests	18
Arsenic (V) and Arsenic (III) Adsorption as a Function of pH	18
Preparation of Fe-GAC through Incipient Wetness Impregnation	19
CHAPTER 3 RESULTS AND DISCUSSION.....	23
Effect of Preparation Temperature on Iron Tailored GAC.....	23

Mini-Column Results.....	23
Arsenic (V) and Arsenic (III) Adsorption as a Function of pH	24
X-ray diffraction (XRD) analysis	25
Cationic Surfactant Loaded Onto Fe-Loaded GAC.....	29
Column Results.....	29
Column tests using Rutland water	31
CHAPTER 4 CONCLUSIONS	35
CHAPTER 5 SIGNIFICANCE TO UTILITIES	37
REFERENCES	39
ABBREVIATIONS	43

TABLES

1.1	pK _a Values of Arsenate and Arsenite	2
1.2	Characteristics of Rutland Groundwater.....	7
1.3	Parameters of kinetic study	15
1.4	Summary of Kinetic Study.....	15
2.1	Media prepared	21

FIGURES

1.1.	Molecular configurations of arsenite and arsenate	3
1.2	(A) arsenate and (B) arsenite speciation as a function of pH	3
1.3	Arsenic removal from drinking water: CTAC loaded SAI Activated Carbon (200×400 Mesh; 9-min full-scale EBCT) and Virgin SAI Activated Carbon (200×400 Mesh; 20-min full-scale EBCT)	6
1.4	Column tests using Rutland water (influent arsenic concentrations: 50–60 $\mu\text{g L}^{-1}$): media (M-1: Fe 3.6%, M-2: Fe 5.4%, and M-3: Fe 6.1%) prepared at 80°C , media loading (1 g), EBCT (0.75 min), the Rutland water pH was adjusted to 6.5 prior to tests.	8
1.5	Column results of media (M-4 with 11% Fe and M-8 with 13.2% Fe): M-4 (media loading: 0.4g, EBCT: 1.07±0.04 min, BVs: 0.77mL), M-8 (media loading: 0.41g, EBCT: 1.01 min, BVs: 0.73 mL), Influent As (V) 300 $\mu\text{g/L}$, HCO_3^- 0.3 mM, and pH 6.5.....	9
1.6	Column results: () M-4 (media loading: 0.4g, EBCT: 1.07±0.04 min, BVs: 0.77mL) and () M-5 [cationic surfactant (Arquad 2C-75)-Fe-SD] (media loading: 0.4g, EBCT: 1.06±0.04 min, BVs: 0.77 mL), Influent As (V) 300 $\mu\text{g/L}$, HCO_3^- 0.3 mM, and pH 6.5.....	10
1.7	Column results: () M-4, influent arsenate (2,000 $\mu\text{g/L}$), EBCT (1.4 min), () M-5 (Arquad 2C-75-Fe-SD), influent arsenate (2,000 $\mu\text{g/L}$) + ClO_4^- (2,000 $\mu\text{g/L}$), EBCT (1.4 min), both influents contained HCO_3^- 0.3 mM, and pH 6.5.....	10
1.8	Kinetic studies of arsenate removal for media M-1, M-2, and M-3. (A) kinetics and fitting lines using pseudo-second order kinetic model, (B) transformation using film and interparticle diffusion equations: open symbols for X and close symbols for F(X), (C) initial sorption rates according to Fe loadings for each medium, (D) adsorption capacities at equilibrium. The operational conditions: arsenate (1 mg/L), media mass (0.1 g), and pH (6.5±0.2).	13
1.9	Kinetic studies of arsenate removal for media, M-4, M-6, and M-7. Figures B and C show the data converted according to equations (1) and (2), respectively. The operational condition: arsenate (3 mg/L), media mass (0.15 g), and pH (6.5±0.2).....	14
1.10	Apparent diffusivity constants according to iron loadings for Fe-GAC 200×400 meshes (), and 80×140 meshes ()	14
2.1	Schematic of hydrous ferric oxide impregnated granular activated carbon	20
2.2	Schematics for Fe-GAC and cationic surfactant [Arquad 2C-75 or Cetylpyridinium chloride (CPC)]-Fe-GAC preparation.....	20

3.1	Column results of media: M-4 (media loading: 0.4g, EBCT: 1.07±0.04 min, BVs: 0.77 mL), M-9 (media loading: 0.26 g, EBCT: 1.09±0.05 min, BVs: 0.75 mL), M-10 (media loading: 0.3 g, EBCT: 1.09±0.04 min, BVs: 0.73 mL), M-11 (media loading: 0.336 g, EBCT: 1.04±0.1 min, BVs: 0.72 mL), M-12 (media loading: 0.375 g, EBCT: 1 min, BVs: 0.73 mL). Influent As (V) 300 µg/L, HCO ₃ ⁻ 0.3 mM, and pH 6.5. M-4, 9, and 10 (Jang et al. 2006b).....	24
3.2	Comparisons of arsenic removal performances based on iron loadings for media (A) treated bed volumes at 50 µg/L breakthrough, (B) arsenate adsorption capacities based on Fe content, (C) arsenate adsorption capacities at 50 µg/L breakthrough based on Fe content. For synthetic water with 300 µg/L As.....	26
3.3	Adsorption edge tests of arsenite and arsenate removal for M-4 (Δ/ , 11%, 80°C, 6h) (Jang et al. 2006b) and M-9 (/ , Fe 7.5%, 60°C, 12h). GAC media concentration (0.1 g/L), arsenic concentrations (3 mg/L), stirring times (1 day).....	27
3.4	XRD results for (A) pure super darco (GAC), (B) M-10 (Fe 9.2%, 60°C, 12h), (C) M-12 (Fe 11.7%, 60°C, 12h), (D) M-4 (Fe 11%, 80°C, 6h), (E) M-8 (Fe 13.2%, 90°C, 4h), , +, and * indicate quartz, akaganéite, and 2-line ferrihydrite (or HFO) peaks, respectively.	28
3.5	Column results: (A) M-10 (Δ), Fe 9.2%, influent arsenate (300 µg/L), M-13 (), Fe 9.2%, (B) perchlorate removal of M-13. All column studies were conducted with the condition: influent arsenate (300 µg/L) and perchlorate (800 µg/L): both influents contained HCO ₃ ⁻ 0.3 mM, and pH 6.5, EBCT 1 min.....	30
3.6	Column results of M-15. The column study was conducted with influent arsenate (300 µg/L) and perchlorate (800 µg/L). Both influents contained 0.3 mM HCO ₃ ⁻ , and pH 6.5, EBCT 1 min.	31
3.7	Arsenic results of column tests using Rutland water for media (M-12: Fe 11.7%) and CPC post-impregnated Fe (11.7%)-SD (influent arsenic concentrations: 60.5 µg/L and spiked perchlorate concentration: 40 µg/L, 100×140 mesh sizes, media loading: 0.44 g, EBCT: 2 min).....	32
3.8	Perchlorate results of column tests using Rutland water for media (M-12: Fe 11.7%) and CPC post-impregnated Fe (11.7%)-SD (influent arsenic concentrations: 60.5 µg/L and spiked perchlorate 40 µg/L, 100×140 mesh sizes, media loading: 0.44 g, EBCT: 2 min).....	33
3.9	Arsenic result of column tests using Rutland water for media (M-14, Fe (12.1%)-SD, arsenic concentration in Rutland water: 60.5 µg/L, 200×400 mesh sizes, loading: 0.84 g, EBCT: 0.75 min).....	33

FOREWORD

The Water Research Foundation (Foundation) is a nonprofit corporation that is dedicated to the implementation of a research effort to help utilities respond to regulatory requirements and traditional high-priority concerns of the industry. The research agenda is developed through a process of consultation with subscribers and drinking water professionals. Under the umbrella of a Strategic Research Plan, the Research Advisory Council prioritizes the suggested projects based upon current and future needs, applicability, and past work; the recommendations are forwarded to the Board of Trustees for final selection. The Foundation also sponsors research projects through the unsolicited proposal process; the Collaborative Research, Research Applications, and Tailored Collaboration programs; and various joint research efforts with organizations such as the U.S. Environmental Protection Agency, the U.S. Bureau of Reclamation, and the Association of California Water Agencies.

This publication is a result of one of these sponsored studies, and it is hoped that its findings will be applied in communities throughout the world. The following report serves not only as a means of communicating the results of the water industry's centralized research program but also as a tool to enlist the further support of the nonmember utilities and individuals.

Projects are managed closely from their inception to the final report by the Foundation's staff and large cadre of volunteers who willingly contribute their time and expertise. The Foundation serves a planning and management function and awards contracts to other institutions such as water utilities, universities, and engineering firms. The funding for this research effort comes primarily from the Subscription Program, through which water utilities subscribe to the research program and make an annual payment proportionate to the volume of water they deliver and consultants and manufacturers subscribe based on their annual billings. The program offers a cost-effective and fair method for funding research in the public interest.

A broad spectrum of water supply issues is addressed by the Foundation's research agenda: resources, treatment and operations, distribution and storage, water quality and analysis, toxicology, economics, and management. The ultimate purpose of the coordinated effort is to assist water suppliers to provide the highest possible quality of water economically and reliably. The true benefits are realized when the results are implemented at the utility level. The Foundation's trustees are pleased to offer this publication as a contribution toward that end.

Roy L. Wolfe, Ph.D.
Chair, Board of Trustees
Water Research Foundation

Robert C. Renner, P.E.
Executive Director
Water Research Foundation

ACKNOWLEDGMENTS

The authors of this report are indebted to the following water utilities, companies, and individuals for their cooperation and participation in this project:

Foundation Project Manager:

Hsiao-Wen Chen

PAC Members:

Thomas J. Sorg, USEPA

Bruce M. Thomson, University of New Mexico

Peter Nathanson, P.E., New Mexico Rural Water Association

Patrick V. Brady, Sandia National Laboratories

American Water Works Company:

Jeff Robinson, Indiana-American Water Co.

Troy Day, California-American Water Co.

Robin Casale, AWWSCo.

Siemens Water Technologies:

James Graham

Douglas Gillen

Cool Sandy Beach Community Water System, Inc., Rutland, MA,

Thomas C. Cook

Also, the authors would like to acknowledge the support and services provided by other affiliated Penn State colleagues, including:

Bob Parette

Adam Redding

EXECUTIVE SUMMARY

OBJECTIVES

The objectives of this study were: (1) to incorporate homogeneously active hydrous ferric oxide into the pores of granular activated carbon (GAC) through an incipient wetness impregnation technique; (2) to evaluate the arsenic adsorption capacities of the media by examining adsorption isotherms, kinetics, and column tests; and (3) to understand the adsorption behavior of the media through physicochemical characterization techniques.

BACKGROUND

Literature has shown that the amorphous hydrous ferric oxide (HFO) form of iron has a high capacity to remove both arsenite and arsenate, compared to other conventional adsorption media. Arsenic adsorption onto iron-tailored GAC is considered to be a promising treatment technology because it is economical and easy to set up, and because the skeletal structure of the GAC will preclude the fragile nature of granular iron media. The driving force of this research was to determine how we could create more effective adsorption sites within a porous carbon support media, and we proposed that this would be important because GAC offers a skeletal strength to the iron, as compared to the relatively fragile nature of granular iron media. This project focused on the synthesis of amorphous hydrous ferric oxide within the pores of GAC as an active sorptive material that can complex both arsenite and arsenate with high adsorption capacities. This project also addresses the development of media preparation methods that are environmentally acceptable, cost-effective, and simple.

APPROACH

We also the GAC with both HFO plus a cationic surfactant to enhance favorable diffusivity of the negatively charged arsenate through the GAC pores that would have a positive charge from the cationic surfactant. We also conducted kinetic tests, As(V) and As(III) adsorption isotherms as a function of pH, column tests, and x-ray diffraction (XRD) measurements. This research also addressed how the Fe precipitation temperature (between 50-90°C) affected iron oxide/hydroxide precipitation within the GAC pores.

RESULTS/CONCLUSIONS

Temperature effect on iron oxide/hydroxide precipitation of iron precursor

1. At similar Fe loadings (10–12%), the results of rapid small scale column tests (RSSCTs) showed obvious differences between media dried at 60°C versus 80–90°C: the media treated at 60°C for 12h had about 3–4 times higher arsenic adsorption capacities than the media treated at 80–90°C.
2. As(V) and As(III) isotherms were conducted over a broad range of pH; and these also showed that the media treated at 60 °C had higher adsorption capacities for both arsenite and arsenate than did media treated at 80-90°C. Some literature has suggested that if an

iron media sorbs as much arsenate as arsenite in the pH 7.5–8.5 range, then the iron might be in the hydrous ferric oxide form. When we preloaded iron at 60°C, we observed equal arsenite and arsenate adsorption at pH 7.6, which empirically validated the other indications that this loading condition formed hydrous ferric oxide.

3. This empirical observation was corroborated with x-ray diffraction (XRD) test results. They indicated that the media treated at 60°C showed the two-line ferrihydrite spectra that are indicative of hydrous ferric oxide, whereas the media treated at higher temperatures contained a higher degree of crystallinity associated with iron oxides, and less HFO.
4. Specifically, the peaks for Fe(II)-Fe-SD (90°C, 4h) indicated a dominant phase of akaganéite, while those for Fe-SD (80°C, 6h) appeared as a mixture of akaganéite and 2-line ferrihydrite.

Post-impregnation of cationic surfactant

1. We post-impregnated positively-charged cationic surfactants (cetyl pyridinium chloride (CPC), or Arquad 2C-75—a blend of several quaternary ammonium surfactants) onto iron-loaded GAC, so as to discern whether these cations would enhance the diffusion rates of the anionic arsenate.
2. These column tests showed a 25–50% enhancement of arsenic removal bed life with these cationic surfactants; and the surfactants also offered high removal of perchlorate.

Column tests using synthetic water

1. Column tests were conducted with a synthetic water that contained 300 µg/L As plus other anions (see below). When the iron was preloaded at 60°C for 12 hours, bed volumes to 50 µg/L As breakthrough were 2–4 times longer than when the iron was preloaded at 80°C or 90°C. Also, preloading CPC or Arquad 2C-75 with the HFO improved bed life.

RSSCTs using Rutland water

1. The media prepared at 80°C treated about 8,000–10,000 BVs before 10 µg/L breakthrough, when the media contained 3.6–6.1% Fe. Without adjusting pH in Rutland water (7.6–8.0), the media treated at lower temperature (50°C) processed about 16,000 BVs before 10 µg/L breakthrough, when the media contained 12.1% Fe. In parallel research under our 3163 Contract, we have achieved 26,000–33,000 bed volumes (BVs) before 10 µg/L arsenic breakthrough. When coupled with zero valent iron solubilization, bed lives of 43,000–150,000 BVs could be reached, as determined in our companion Contracts 3163 and 3013.

Addition effect of citrate ions for iron precursor

1. The kinetic results show all data fit well with an intraparticle diffusion model, indicating that the rate limiting step for arsenate removal was pore diffusion.
2. Although the increase of iron loadings might raise the apparent diffusivity constants, the addition of citric acid did not have a synergetic effect with iron to remove arsenate under

the conditions that we tested (i.e. a 80–90°C precipitation temperature). Subsequent tests may appraise the benefits of citrate when using a 60°C precipitation temperature.

APPLICATIONS/RECOMMENDATIONS

Compared to conventional Fe oxide media that are synthesized by the sol-gel process, the method for preparing iron-tailored GAC is more environmentally acceptable, cost-effective, and simple due to less preparation steps and small uses of Fe precursor. Moreover, there needs be no waste left after media synthesis. Additionally, a cationic surfactant post-impregnated HFO-GAC has a high potential in remediating groundwater that contains both arsenic and perchlorate because of its simultaneous removal mechanism.

In future and ongoing research, we aim to improve the arsenic adsorption of iron-tailored media yet further, by accumulating yet more hydrous ferric oxide within the GAC pores that is yet more dispersed, more nano-grained, and with higher surface area. To reach this objective, we will continue to investigate the arsenic removal mechanism for hydrous ferric oxide that is incorporated into activated carbon. We will address the underlying issues of this by employing several spectroscopic analysis protocols (FT-IR, XPS, XRD, XAS, etc.), and by employing surface complexation modeling. We are also developing a pilot-scale media preparation protocol so that we can apply the media in pilot-scale arsenic removal trials.

PARTICIPANTS

- American Water Works Company
- Cool Sandy Beach Community Water System
- Siemens Water Technologies

CHAPTER 1

INTRODUCTION

BACKGROUND

Throughout the world, arsenic is creating potentially serious environmental problems for humans and other living organisms. Most reported arsenic problems are found in groundwater water supply systems and are caused by natural processes such as mineral weathering and dissolution resulting from a change in the geo-chemical environment to a reductive condition (Namasivayam and Senthilkumar 1998, Chris et al. 2000). Arsenic contamination is also caused by human activities such as mining wastes, petroleum refining, sewage sludge, agricultural chemicals, ceramic manufacturing industries and coal fly ash (Grossl et al. 1997, Manning and Goldberg 1997, Viraraghavan et al. 1999).

Millions of people in Western Bengal and Bangladesh have been drinking groundwater from wells that contain 100-2,000 $\mu\text{g/L}$ As, and many of these people have succumbed to diseases that are caused by the arsenic contaminated ground water (Mandal et al. 1996). In the United State, Smith et al. (1992) reported that over 35,000 people may be drinking water contaminated with more than 50 $\mu\text{g/L}$ of arsenic and over 2.5 million people could be supplied with water having arsenic levels over 25 $\mu\text{g/L}$. Consumption of arsenic at the 50 $\mu\text{g/L}$ level is estimated to cause mortality due to lung, kidney, or bladder cancer in 1 out of every 1,000 or 10,000 people. The World Health Organization (WHO) announced that water containing more than 50 $\mu\text{g/L}$ of arsenic is unsuitable due to acute and chronic toxicity. Owing to epidemiological evidence linking arsenic and cancer, the safe limit of arsenic in drinking water was reduced from 50 $\mu\text{g/L}$ to 10 $\mu\text{g/L}$ in 1993 by WHO (Tokunaga et al. 1999, Johnston and Heijnen 2001). The Clinton administration promulgated a new maximum concentration level (MCL) of 10 $\mu\text{g/L}$ As, and the EPA announced on October 31, 2001 that public water supplies nationwide should reduce arsenic concentration levels to below 10 $\mu\text{g/L}$ by 2006. Complying with these stringent limits on arsenic will impose a heavy financial burden on small public water system (Woods 2001). The **objective** of this research has been to discern a less expensive means of removing arsenic from groundwater, particularly for small municipalities. Compared to conventional Fe oxide media that are synthesized by the sol-gel process, the method of preparing iron tailored GAC herein is more environmentally acceptable, cost-effective, and simple; due to fewer preparation steps and less iron precursor. Moreover, there need be no waste left after media synthesis.

CHEMISTRY OF ARSENIC

Arsenic Immobilization

Arsenic is of concern in water treatment because of its health effects. In general, inorganic arsenic compounds are more toxic than organic arsenic compounds, and arsenite [As(III)] is more toxic than arsenate [As(V)]. The molecular structure of both arsenate and arsenite are shown in Figure 1.1. The double-bonded oxygen in arsenate has a large effect on the ionization due to the loss of hydrogen ions. The tendency of ionization is expressed by pK_a (the dissociation constant). For arsenic species, acid-base equilibria and pK_a values are summarized

in Table 1.1. Figure 1.2 shows a schematic of the pH relationship between arsenic species and illustrates the significant difference in the pH values of ionization steps that occur between arsenate and arsenite. The pE-pH relationship is important for understanding the mobility of arsenic species in groundwater and the effectiveness of arsenic treatment systems (Sun and Doner 1998). Inorganic arsenic species mainly exist in the +3 or +5 oxidation state. These oxidation states are controlled by micro-organisms, redox potential, and pH, as well as reactions with other chemical compounds in the soil and sediments such as iron sulfides, iron/manganese/aluminum oxides and hydroxides, dissolved organic matter, etc. (Loeppert et al. 1995).

Components of soils and sediments are involved with ionic species in two types of adsorptive reactions. The first type of adsorption reaction is based on ion exchange between charged adsorptive sites and charged soluble ions. The second type is London Van der Waals bonding and is the result of complex interactions between the electron clouds of molecules, molecular polarity, and the attractive forces of an atomic nucleus for electrons beyond its own electron cloud. The change of groundwater to a reductive condition could cause the arsenate attached in the soil or sediment to be released into the liquid phase due to the chemical reduction of arsenate to arsenite (especially predominant species H_3AsO_3 at below pH 9.22), which is more mobile due to its weak adsorption on most mineral surfaces (Scott 1991, Manning and Goldberg 1997). The redox alterations incurred when drawing reduced groundwater out of the ground can increase the arsenic levels in the extracted water.

Table 1.1
pK_a Values of Arsenate and Arsenite

Species	Acid-base equilibria	pK _a
Arsenate (Arsenate)	$\text{H}_3\text{AsO}_4 \longleftrightarrow \text{H}_2\text{AsO}_4^- + \text{H}^+$	2.20
	$\text{H}_2\text{AsO}_4^- \longleftrightarrow \text{HAsO}_4^{2-} + \text{H}^+$	6.97
	$\text{HAsO}_4^{2-} \longleftrightarrow \text{AsO}_4^{3-} + \text{H}^+$	11.53
Arsenite (As(III))	$\text{H}_3\text{AsO}_3 \longleftrightarrow \text{H}_2\text{AsO}_3^- + \text{H}^+$	9.29
	$\text{H}_2\text{AsO}_3^- \longleftrightarrow \text{HAsO}_3^{2-} + \text{H}^+$	12.10

Speciation

Arsenic in solution can be present as the semi-metallic element (As^0), arsenate (As^{5+}), arsenite (As^{3+}), arsine (As^{3-}), monomethylarsonate (MMAA), and dimethylarsinate (DMAA). The amount of each of these species depends on the redox conditions and the nature of anthropogenic input and biological activity. However, the organic (methylated) arsenic usually occurs at natural concentrations of less than 1 µg/L and is not of major significance in drinking water treatment (Edwards 1994). Arsenate (as H_2AsO_4^- and HAsO_4^{2-}) is the predominant and stable inorganic arsenic form in the oxygen-rich aerobic environments (well-oxidized waters), while arsenite occurs primarily as H_3AsO_3^0 and H_2AsO_3^- (above pH 9.3) in reducing anaerobic

environments. Due to the relatively slow redox transformation, both arsenite and arsenate are often found in either redox environments (Scott and Morgan 1995, Viraraghavan et al. 1999).

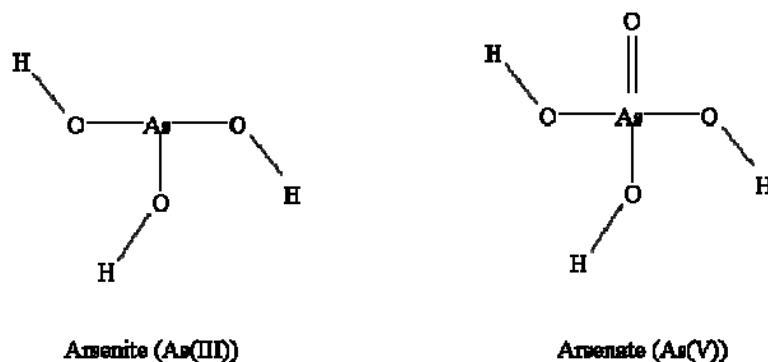


Figure 1.1. Molecular configurations of arsenite and arsenate

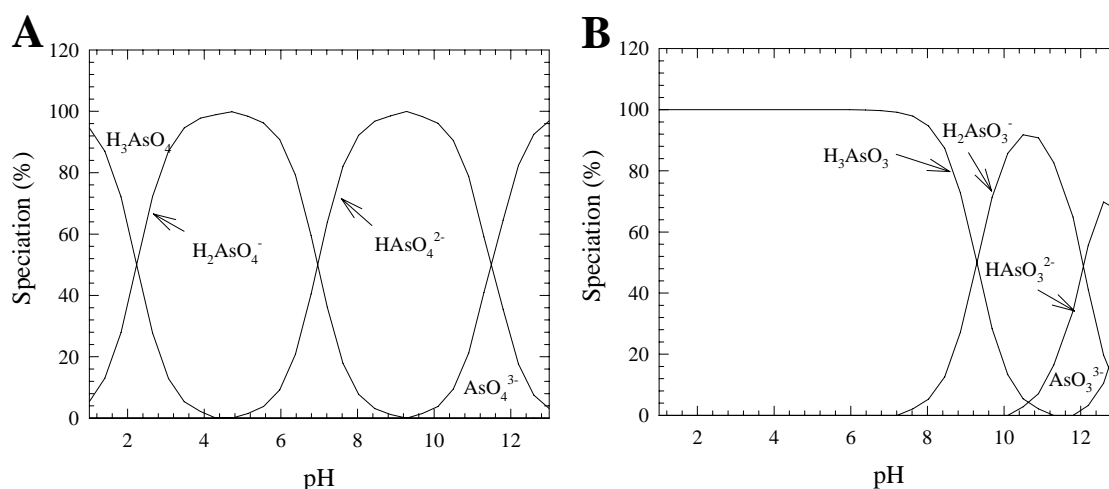


Figure 1.2 (A) arsenate and (B) arsenite speciation as a function of pH

ARSENIC ADSORPTION TECHNOLOGIES

Compared to other conventional techniques such as oxidation, coagulation/precipitation, filtration, ion exchange, membrane/reverse osmosis, and biological treatments, adsorption has the following advantages: (1) it usually does not need a large volume or additional chemicals for treatment; (2) it is easier to set up as a POE/POU (Point of Entry/Point of Use) arsenic removal process. Activated alumina has been extensively studied because it is very effective and selective for arsenic adsorption removal (Gilles 2000). Activated alumina is also useful for high TDS water. However, it is very sensitive to pH. The optimum pH is 5.5–6.0 to achieve an optimum arsenic adsorption capacity (Chwirka et al. 2000). In addition, after activated alumina is regenerated, its adsorption capacity is reduced by 20–50%. The chemicals used for pH adjustment and bed regeneration, such as sulfuric acid and sodium hydroxide, can be large

burdens, requiring sensitive and often expensive equipment for process control. Once acid is added to lower pH to an optimum condition, the reverse action to increase the pH of the effluent should be performed to avoid corrosion problems. A highly concentrated brine waste stream produced after regeneration is another problem.

Other adsorption materials have been tried for arsenic removal. Namasivayam and Senthilkumar (1998) studied wasted Fe(III)/Cr(III) hydroxide as a non-conventional adsorbent for the removal of arsenic from wastewater. Suzuki et al. (2000) investigated the adsorption of oxo-anions, such as arsenic and selenium, onto a polymer adsorbent in which a Zr(IV)-EDTA complex was immobilized. They discovered that common anions such as sulfate, chloride, nitrate, and acetate did not interfere with the oxo-anion adsorption onto the Zr(IV)-EDTA impregnated polymer. Reed et al. (2000) studied arsenite, arsenate, mercury, and lead removal by iron-impregnated activated carbon. Haron et al. (1999) studied the arsenic adsorption from an aqueous solution with the iron(III)-poly(hydroxamic acid) resin complex. The complex was most effective at a pH range of 2.0 to 5.5, and other anions such as chloride, nitrate, and sulphate did not have detrimental effects on the arsenic adsorption for the complex media. Manju et al. (1998) used copper impregnated coconut husk carbon for the arsenite removal in synthetic and industrial wastewaters. Its adsorption capacity was found to increase with increasing pH and a maximum capacity was attained at pH 12. Min and Hering (1998) studied arsenic removal by the use of biopolymer alginic acid pretreated with calcium and iron (III). The Ca-Fe beads showed effective arsenic adsorption efficiencies; however, it was critical that the pH condition be at the optimum 4.0. In addition, the iron can easily leach out with an increase in pH. Pal (2001) described the arsenic adsorption of granular ferric hydroxide (GFH). GFH, a poorly crystallized α -FeOOH, has a high arsenic adsorption capacity and good selectivity. Pal explained that these good adsorption results were caused by the high density of available adsorption sites. This was achieved in the synthesis method by which water remained in the adsorption sites. Jang et al. (2006) studied the HFO impregnation onto diatomite and identified the formation of HFO through several surface characterization studies and surface complexation modeling works.

As additional recent information, Siegel et al. (2006) comprehensively reviewed recently-developed adsorption materials: metal oxhydroxide adsorbents, coated synthetic materials, coated natural materials and waste products, as well as other innovations to improve media performance.

HYDROUS FERRIC OXIDE (HFO) INCORPORATED GRANULAR ACTIVATED CARBON

The authors herein offer adsorption onto iron-tailored GAC as a promising technology because it is economical and easy to set up, and because the skeletal structure of the GAC will offer a strong sheath around the fragile iron hydroxides. For the research herein, we focused on a synthesis method for implanting amorphous hydrous ferric oxide (HFO) into the pores of GAC. We offered this as an active sorptive material that can complex both arsenite and arsenate with high adsorption capacities. We also developed media preparation methods that are effective, environmentally acceptable, inexpensive, and simple. Our work on impregnating HFO into activated carbon has built on the work of others. HFO has been extensively studied as a promising adsorptive material for removing both arsenate and arsenite from the aqueous phase due to its high iso-electric point (IEP 8.1) and high surface area (Raven et al. 1998, Dixit and Hering 2003, Jang et al. 2006a), and selectivity for arsenic species. Since HFO has high energy

sites that could be complexed specifically with arsenite, it has high affinities for arsenite (Jackson and Miller 2000).

These earlier studies appraised HFO in media other than GAC. Iron oxides that include HFO are generally made as suspensions in an aqueous solution that are not suitable for column applications due to their low hydraulic conductivity (Zeng 2003). To overcome this disadvantage, others have developed HFO granulation techniques, which are susceptible to crumbling. Those other authors synthesized granular ferric hydroxide (GFH) from ferric chloride solution by neutralization and precipitation with sodium hydroxide, followed by centrifugation and granulation under high-pressure (Thirunavukkarasu et al. 2003a, Gu et al. 2005). However, GFH has traditionally shown poor mechanical strength, and crumbles into fine particles that increase headlosses (Gu et al. 2005). There are several trials of developing adsorption media with different types of porous hosting materials such as polymer (Cumbal et al. 2003, Cumbal and SenGupta 2005), sand (Thirunavukkarasu et al. 2003b, Vaishya and Gupta 2003), GAC (Gu et al. 2005), and diatomaceous earth (Jang et al. 2006a). However, their Fe-coated materials were less effective and/or sturdy than what the authors herein have aimed to develop. To overcome these disadvantages of GFH or other Fe-coated media, our team developed an incipient wetness impregnation method, which highly disperses and incorporates HFO homogeneously in the pores of GAC using a rotary evaporator. Compared with the preparation methods of other media, this technique is simple because fewer steps and a small volume of precursor solution are needed for media preparation. In addition, there is no iron solution remaining in excess that should be treated.

EFFECT OF CITRATE ION ADDITION ON IRON PRECURSORS

Several authors have observed that the citrate ion influences the formation of several different types of iron oxide such as α -FeOOH, β -FeOOH, and γ -FeOOH (Kandori et al. 1991, Ishikawa et al. 1993). Kandori et al. and Ishikawa et al. found that the addition of specific molar portion of citrate ions into iron precursors can not only form nano-scale particles of iron oxides, but also increase specific surface areas. This is because citrate ions can inhibit the formation and crystallization of iron oxide particles. Their results also showed that citrate addition higher than 2 mol % (percentage of molar ratio between citrate and Fe) could create significant aggregations of amorphous particles. Our hypothesis was that the presence of citric ions during the formation of iron oxide could help create nano-scale iron oxide particles; and these nano particles could have higher specific surface area and increased adsorption site densities for negatively-charged arsenic species.

EFFECT OF TEMPERATURE ON PREPARATION OF IRON MODIFIED GAC

We sought to discern the most favorable temperature for preparing iron oxide/hydroxide precipitates. This work has been prompted in part by observing that Kandori et al. (1991) and Ishikawa et al. (1993) prepared amorphous iron oxides with low temperatures; and we thus compared results of Fe-GAC media prepared at 50–90°C temperature ranges (see below).

CATIONIC SURFACTANT LOADED ONTO FE-INCORPORATED GAC

Several researchers have observed that cationic functional groups on the polymer aid the diffusion of anions through media via the Donnan membrane effects, and so the authors herein have tested whether this mechanism would also aid arsenic removal. This work has built on our Penn State work, funded through other Foundation projects, where we have been preloading cationic surfactants onto GAC to remove perchlorate (ClO_4^-) from groundwater (Parette and Cannon 2005, Parette et al. 2005). The removal mechanism of perchlorate with cationic surfactants is likely based on ion exchange. This is different from the surface complexation mechanism, on which arsenic removal mostly depends. Our RSSCT test showed that when the cationic surfactant cetyltrimethylammonium chloride (CTAC) was preloaded onto GAC, it exhibited poor arsenic removal (Figure 1.3). However, both CTAC and CPC exhibited excellent perchlorate removal (Parette and Cannon 2005).

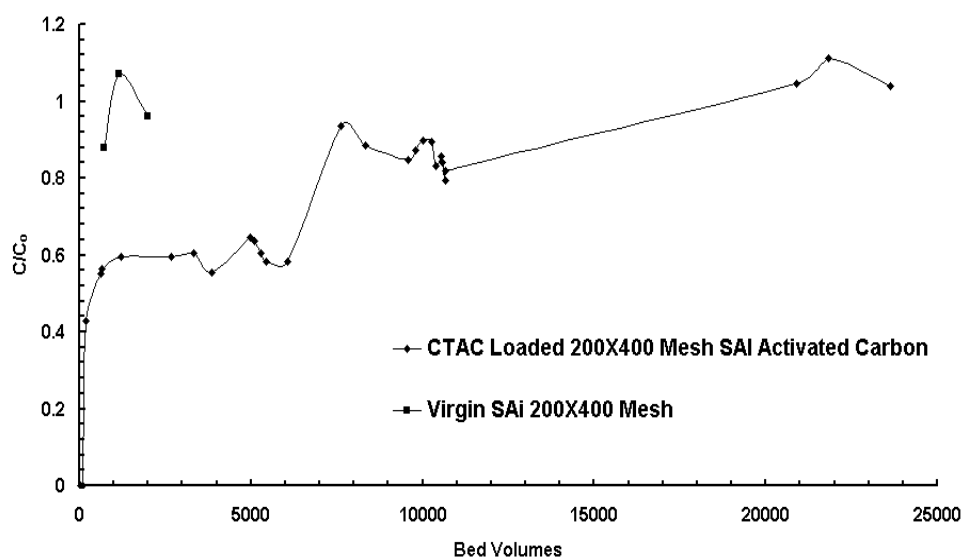


Figure 1.3 Arsenic removal from drinking water: CTAC loaded SAI Activated Carbon (200×400 Mesh; 9-min full-scale EBCT) and Virgin SAI Activated Carbon (200×400 Mesh; 20-min full-scale EBCT)

Recent study by Cumbal and SenGupta (2005) have shown that cationic functional groups on the surface of a membrane can attract negatively-charged species such as arsenic and thereby concentrate arsenic species in the pore phase. In our study, we attempted to use GAC as a host material for these cationic surfactants so as to achieve a similar Donnan-effect enhancement of anionic arsenic diffusion into GAC-iron pores.

OBJECTIVES

The objectives of this study were: (1) to incorporate homogeneously active hydrous ferric oxide into the pores of GAC through an incipient wetness impregnation technique; (2) to evaluate the arsenic adsorption capacities of the media produced by examining As(V) and As(III)

adsorption isotherms, kinetics, and rapid small-scale column tests (RSSCTs); and finally (3) to understand the adsorption behavior of the media through physicochemical characterization techniques.

PRIOR AND PARALLEL RESEARCH AT PENN STATE

Column Tests Using Rutland Groundwater

To discern arsenic removal performance of developed media in natural groundwater, column tests were conducted using Rutland water, of which the characteristics were as presented in [Table 1.2](#). This natural groundwater contained 50–60 µg/L of arsenic and about 13 mg/L of silica. The silica could give a competition effect with arsenic in these iron-based media.

Table 1.2
Characteristics of Rutland Groundwater

pH	Iron, µg/L	Hardness (mg/L) as CaCO ₃	TOC, (mg/L)	Na, (mg/L)	Mg, (mg/L) as CaCO ₃	Cl (mg/L)	Sulfate, (mg/L)	Silica (mg/L)	Ca (mg/L) as CaCO ₃	Turbidity (NTU)
7.6–8.0	3	70.3	0.85	27.5	11.3	9.3	26.4	12.5	59	0.08

Several column results using Rutland water have been presented in [Figure 1.4](#); and the descriptions of the media are as presented in [Table 2.1](#) below. A media prepared at 80°C with 5.4% iron loading (designated as M-2) was able to treat about 10,000 bed volumes (BVs) before 10 µg/L As breakthrough, while a media prepared at 80°C with citrate (2 mol % based on the mole of Fe) and 6.1% Fe loading (designated as M-3) could treat 9,000 BVs to 10 µg/L breakthrough, and a media prepared at 80°C with 3.6% Fe loading (designated as M-1) could treat about 8,000 BVs. respectively (Please see the [Table 2.1](#)). These results were obtained at an adjusted pH of 6.5.

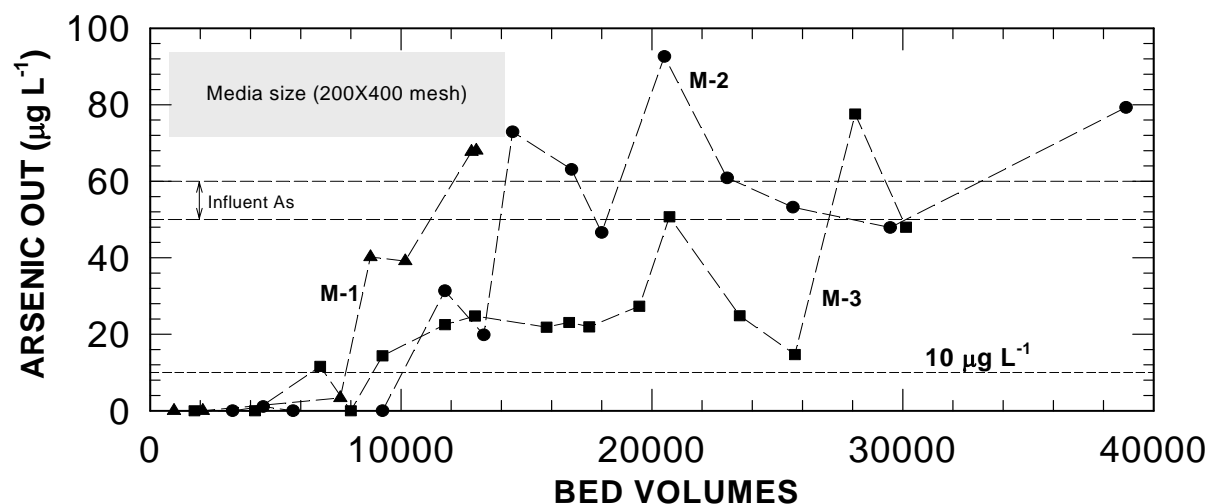


Figure 1.4 Column tests using Rutland water (influent arsenic concentrations: 50–60 $\mu\text{g L}^{-1}$): media (M-1: Fe 3.6%, M-2: Fe 5.4%, and M-3: Fe 6.1%) prepared at 80°C, media loading (1 g), EBCT (0.75 min), the Rutland water pH was adjusted to 6.5 prior to tests.

Sequential Incipient Wetness Impregnation of Ferrous onto Fe-GAC

In order to test a wide array of media in a shorter time frame, the authors employed a synthetic water that contained 300 $\mu\text{g/L}$ of arsenic and background buffering; and tested bed volumes to breakthrough with 1-mL syringe mini-columns. These mini-columns had a 6 mm diameter and 10 cm length, and their empty bed contact times (EBCTs) ranged from 0.8–2 min. A 1 min EBCT was mainly used for the media of 100×140 (median: 125 μm) and 80×140 (median: 136 μm). In accordance with the proportional diffusivity similitude (Parette and Cannon 2005), the mini-column tests with 1 min EBCT (100×140 mesh) simulated an EBCT of 8.4 minutes for US mesh #12×40 (1700–425 μm ; median 1060 μm) full-scale media, or 3.5 minutes for US mesh #20×50 (850–300 μm ; median 440 μm). Synthetic arsenic-containing water was prepared for column tests with DI water, in which 0.3 mM NaHCO_3 , 0.01 M NaCl , 300–2,000 $\mu\text{g/L}$ arsenate, and 0–2,000 $\mu\text{g/L}$ perchlorate were respectively added. Using 0.1 M of NaOH or HCl , the pH of synthetic water was kept at 6.5 ± 0.2 .

Through sequential incipient wetness impregnation of ferrous chloride for iron tailored Superdarco (designated as M-8, Fe(II)-Fe-SD, see Table 2.1), we attempted to increase the iron loadings. The iron loading percentage for Fe(II)-Fe-SD was increased to 13.2%. Figure 1.5 shows the column results of iron tailored Superdarco (designated as M-4, Fe 11%) and Fe(II)-Fe-SD (Fe 13.2%, M-8) when treating a synthetic water that contained 300 $\mu\text{g/L}$ arsenate. By employing a complete drying step under the hood before the Fe precipitation step, we could get higher a Fe content than for the previous cases described above (Fe 3.6–6.1%).

The media that contained 11% and 13.2% iron exhibited had similar arsenic breakthroughs at 1,500 BVs; and this meant that the media with the lesser amount of iron was the more efficient, on a mg As / g Fe basis, at removing arsenic. The media with 13.2% Fe had been

prepared at 90oC, and as will be discussed in Chapter 3, this higher precipitation temperature yielded a more crystalline form of iron.

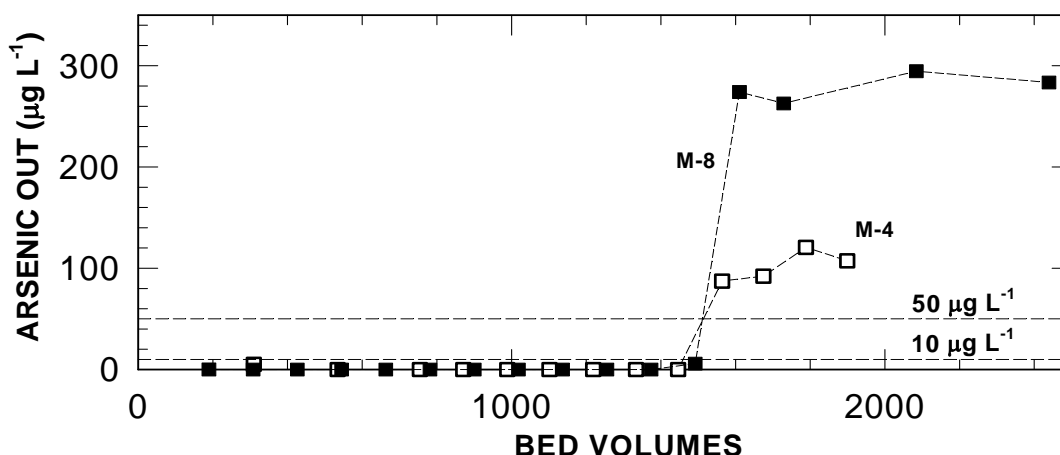


Figure 1.5 Column results of media (M-4 with 11% Fe and M-8 with 13.2% Fe): M-4 (media loading: 0.4g, EBCT: 1.07 ± 0.04 min, BVs: 0.77mL), M-8 (media loading: 0.41g, EBCT: 1.01 min, BVs: 0.73 mL), Influent As (V) 300 µg/L, HCO_3^- 0.3 mM, and pH 6.5.

Cationic Surfactant Loaded onto Fe-incorporated GAC

As a further opportunity, we also co-loaded the GAC with a cationic surfactant. Our aim was to enhance diffusivity of the negatively charged arsenate through the GAC pores that would have a positive charge from the cationic surfactant. Figures 1.6 and 1.7 show the column results when using a GAC that had been pre-loaded with both Fe, and then a cationic surfactant (Arquad 2C-75) (designated as M-5 with 10.7% Fe). With a 300 µg/L influent As concentration, the media that had been co-loaded with cationic surfactant exhibited 50 µg/L As breakthrough at 2,200 BVs, compared to 1,500 BVs for the media that had no surfactant (Figure 1.6). Therefore, the cationic surfactant enhanced performance by 30–40%.

This test was repeated with an influent arsenic concentration of 2000 µg/L plus an influent perchlorate concentration of 2000 µg/L; and in this case, when the cationic surfactant was present, 50 µg/L As breakthrough occurred at 1,350 BVs, whereas when the cationic surfactant was not present, 50 µg/L As breakthrough occurred at 900 BVs. These media had all been precipitated at 80oC, and similar tests were repeated with media that had been prepared at 60oC, as presented in Chapter 3.

Kinetic Studies

Kinetic studies offer a very good tool to estimate several valuable parameters such as adsorption capacity, initial adsorption rate, and the effective diffusion constant. In this study, a series of media (M-1, M-2, and M-3: 200×400 mesh size) and (M-4, M-6, and M-7: 80×140 mesh size) were used for kinetic tests to discern the effect of citrate acid addition for the

formation of iron oxide and arsenic removal efficiencies (please see the Table 2.1 for media identification).

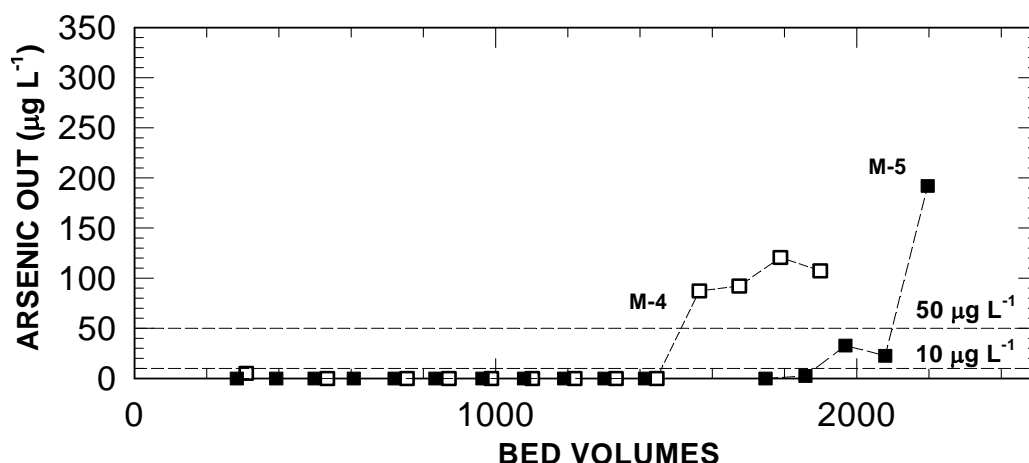


Figure 1.6 Column results: (□) M-4 (media loading: 0.4g, EBCT: 1.07 ± 0.04 min, BVs: 0.77mL) and (■) M-5 [cationic surfactant (Arquad 2C-75)-Fe-SD] (media loading: 0.4g, EBCT: 1.06 ± 0.04 min, BVs: 0.77 mL), Influent As (V) 300 µg/L, HCO_3^- 0.3 mM, and pH 6.5.

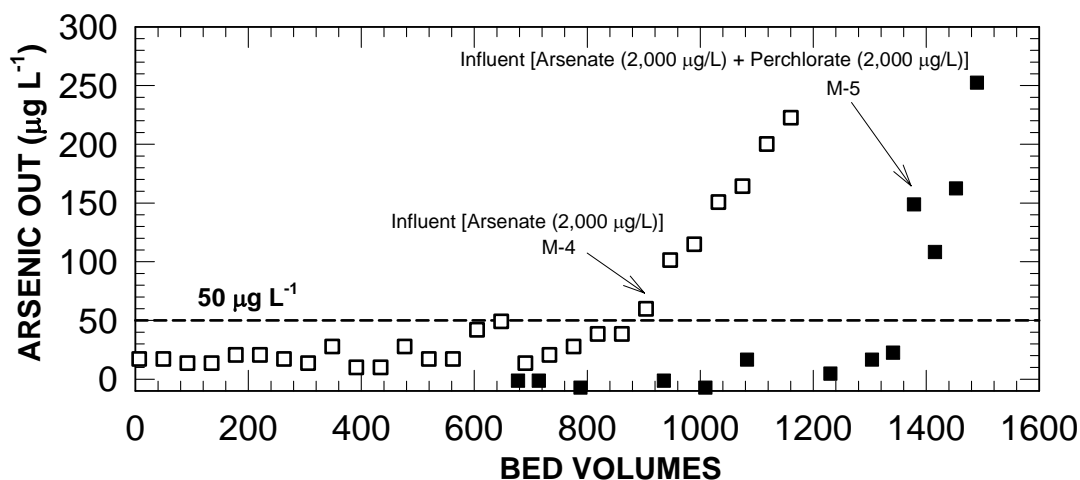


Figure 1.7 Column results: (□) M-4, influent arsenate (2,000 µg/L), EBCT (1.4 min), (■) M-5 (Arquad 2C-75-Fe-SD), influent arsenate (2,000 µg/L) + ClO_4^- (2,000 µg/L), EBCT (1.4 min), both influents contained HCO_3^- 0.3 mM, and pH 6.5.

The pseudo second-order kinetic equation has been found by others to fit well to chemisorption data when using heterogeneous materials (Reddad et al. 2002). With this in mind, the authors herein fitted the kinetic data from several experiments with a pseudo second-order kinetic model, so as to estimate the rate constants, initial sorption rates, and arsenic adsorption

capacities of these different media. The kinetic rate equation is expressed as (Ho and McKay 1998, Reddad et al. 2002):

$$\frac{dq_t}{dt} = k_2 (q_{eq} - q)^2 \quad (\text{Equation 1})$$

Where q_{eq} is the adsorption capacity at equilibrium, and q is the solid phase loading of arsenate. The k_2 ($\text{g} \cdot \text{mmol}^{-1} \cdot \text{min}^{-1}$) is the pseudo-second order rate constant for the kinetic model. By integrating equation 1 with the boundary conditions of $q = 0$ (at $t = 0$) and $q = q_t$ (at $t = t$), the following linear equation can be obtained:

$$\frac{t}{q} = \frac{1}{v_0} + \frac{1}{q_{eq}} t \quad (\text{Equation 2})$$

$$v_0 = k_2 \times q_{eq}^2 \quad (\text{Equation 3})$$

where, v_0 ($\text{mmol g}^{-1} \cdot \text{min}^{-1}$) is the initial sorption rate. Therefore, the v_0 and q_{eq} values of kinetic tests can be determined experimentally by plotting t versus t/q_t .

Along with the pseudo second-order kinetic model, others have used the shrinking core model (Rao and Gupta 1982) to estimate mass-transfer characteristic parameters of arsenic removal. This model assumes that the arsenic adsorption is a fast reaction relative to the diffusion rate steps (Jang et al. 2006a). When considering external film diffusion and intraparticle diffusion control, scientists have used this model to find the apparent diffusivity of metal ions in various adsorbents (Rao and Gupta 1982, Veglio et al. 1998, Seki and Suzuki 1999). For a process controlled by the diffusion of arsenic through the liquid film (film diffusion control), the extent of the arsenic adsorption as a function of time will be given by the following expression.

$$X = \frac{3D_{app}}{\delta RC} \int_0^t C dt \quad (\text{Equation 4})$$

where X denotes the fraction of the arsenic adsorbed to the adsorbent; C (mol/mL) is the concentration of arsenic in the solution, and C^0 (mol/mL) is the initial arsenic concentration at the beginning of the adsorption. D_{app} (cm^2/sec), δ (cm), R (cm), and t (sec) are the apparent diffusivity of arsenic, liquid film thickness, average radius of adsorbent particles, and time, respectively. If the process is controlled by the diffusion through the reacted shell (particle diffusion control), the model is represented by the following expression.

$$f(X) = 1 - 3(1 - X)^{2/3} + 2(1 - X) = \frac{6D_{app}}{R^2 C^0} \int_0^t C dt \quad (\text{Equation 5})$$

$f(X)$ is a function of X . Consequently, a plot of either X vs. $\int_0^t C dt$ or $f(X)$ vs. $\int_0^t C dt$ will show a linear relationship. The apparent diffusivity of the media could be obtained from the slope of such a plot as follows:

$$D_{app} = (\text{slope})C^0 \frac{R^2}{6} \quad (\text{Equation 6})$$

The authors herein used both of these models for characterizing the apparent diffusivities. As shown in [Figures 1.8 and 1.9](#), when the 2 mol % citrate was added to Fe-GAC media, this apparently enhanced arsenic removals. However, an enhanced arsenic removal was also associated with a higher level of iron preloading. As a result it is still not proven that the addition of citrate alone increased the adsorption capacity for arsenic. Also, these tests all used a precipitation temperature of 80–90°C; and the authors subsequently learned that lower precipitation temperature (i.e. 60°C) enhances arsenic removals (see Chapter 3).

[Figures 1.8 and 1.9](#) show that all data fit very well with the pseudo-second order kinetic model. For the media size (200×400 mesh), initial sorption rates and adsorption capacities at equilibrium increased linearly with an increase of iron loadings ([Table 1.3 and 1.4](#)). There is no clear relationship between citrate ion presence and iron loading or effective diffusivity ([Figure 1.10](#)). The increased adsorption characteristics might be mainly due to the higher loadings of iron oxide, rather than any phase change of iron oxide that was caused by adding citrate ions.

The kinetic results showed that all data closely fit the model based on intraparticle diffusion control ([Figure 1.8 \(B\)](#) and [Figure 1.9 \(C\)](#)) rather than the film diffusion control. One may infer from these data that the governing mechanism for arsenate removal is pore diffusion.

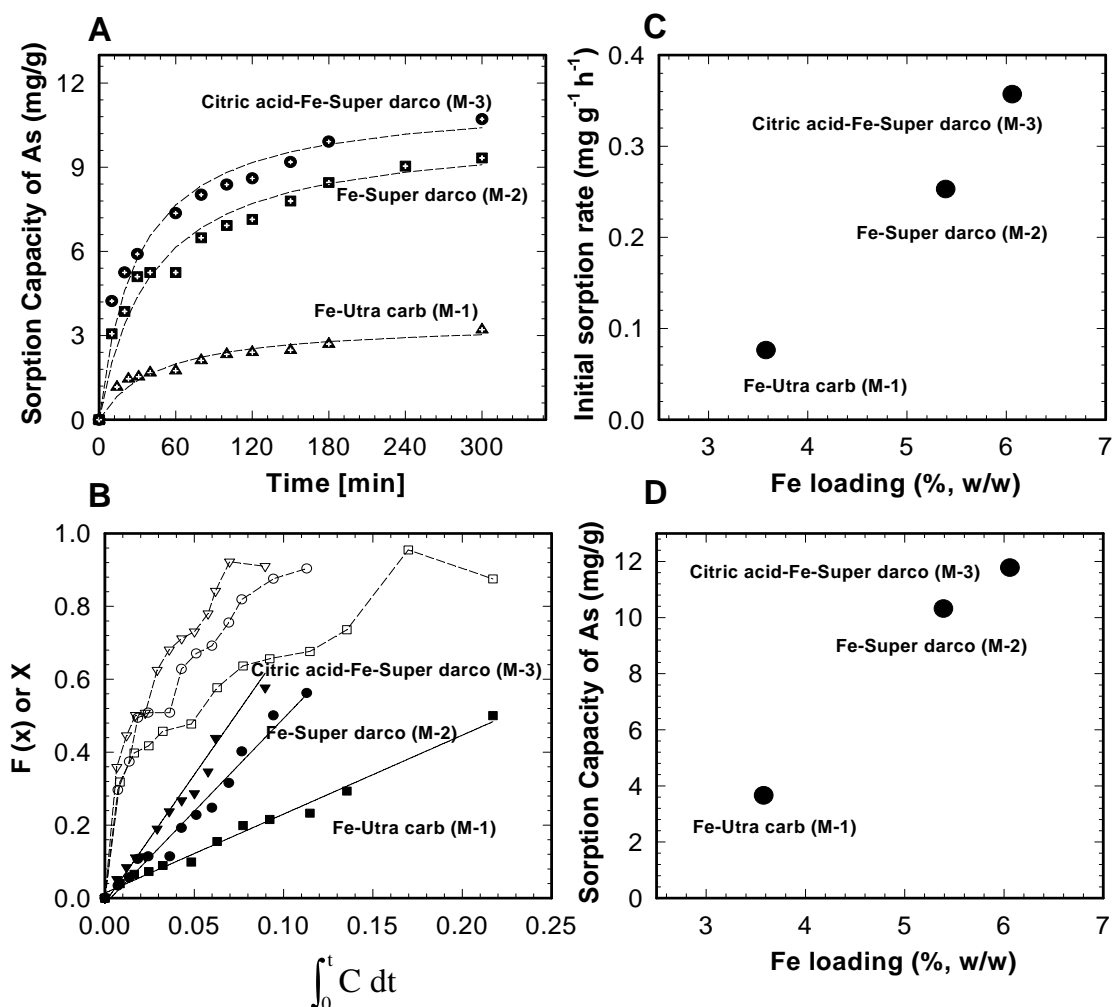


Figure 1.8 Kinetic studies of arsenate removal for media M-1, M-2, and M-3. (A) kinetics and fitting lines using pseudo-second order kinetic model, (B) transformation using film and interparticle diffusion equations: open symbols for X and close symbols for F(X), (C) initial sorption rates according to Fe loadings for each medium, (D) adsorption capacities at equilibrium. The operational conditions: arsenate (1 mg/L), media mass (0.1 g), and pH (6.5 ± 0.2).

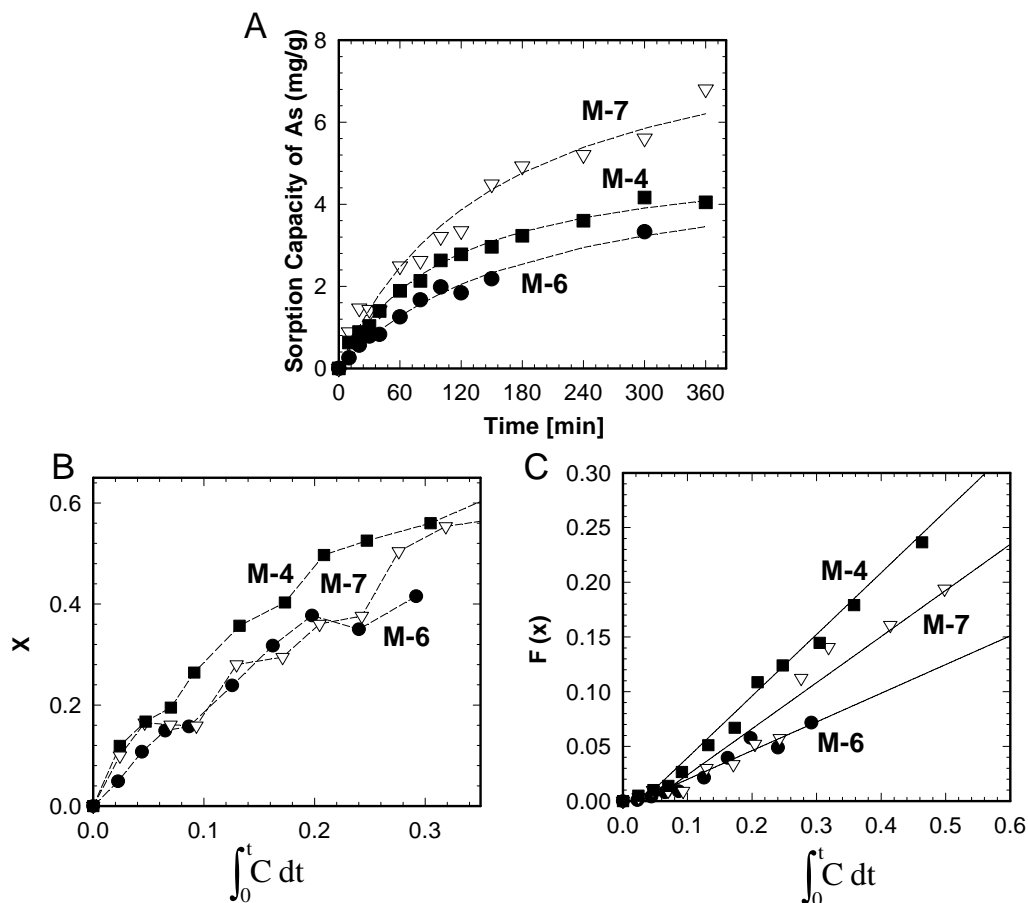


Figure 1.9 Kinetic studies of arsenate removal for media, M-4, M-6, and M-7. Figures B and C show the data converted according to equations (1) and (2), respectively. The operational condition: arsenate (3 mg/L), media mass (0.15 g), and pH (6.5±0.2)

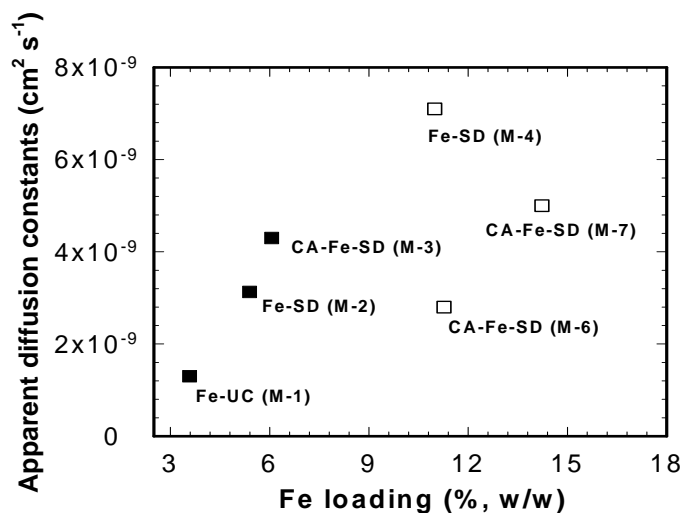


Figure 1.10 Apparent diffusivity constants according to iron loadings for Fe-GAC 200×400 meshes (■), and 80×140 meshes (□)

Table 1.3
Parameters of kinetic study

ID	Media	Pseudo-second order kinetic model				Shrinking core model		
						Pore diffusion		Film diffusion
		v_0^*	q_{eq}^\dagger	$k^2\ddagger$	R^2	R^2	$D_{app}§$	R^2
M-4	Fe-SD	0.0498	5.29	0.00178	0.941	0.959	7.56×10^{-9}	0.882
M-6	CA-Fe-SD (1mL/g)	0.0279	5.26	0.001	0.899	0.920	2.99×10^{-9}	0.913
M-7	CA-Fe-SD (1.5 mL/g)	0.0569	8.90	0.00072	0.984	0.915	5.36×10^{-9}	0.811

* Initial sorption rate ($\text{mg g}^{-1} \text{h}^{-1}$)

† Sorption capacity at equilibrium (mg g^{-1})

‡ The pseudo-second order rate constant for the kinetic model ($\text{g mg}^{-1} \text{h}^{-1}$)

§ Apparent diffusivity ($\text{cm}^2 \text{s}^{-1}$)

Table 1.4
Summary of Kinetic Study

Media	Fe loadings (%)	Fe/As (g/g)	Median size (μm)	Apparent Diffusivity D_{eff} (cm^2/sec)	Adsorption capacities of media (mg As / g media)	Arsenic adsorption densities (mg As/ g Fe)
M-1	3.6	3.58	52.3	1.3E-9	3.66	102.2
M-2	5.4	5.39	52.3	3.1E-09	10.32	191.5
M-3	6.1	6.06	52.3	4.3E-09	11.78	194.4
M-4	11.0	5.50	136.3	7.1E-09	5.29	32.1
M-6	11.3	5.64	136.3	2.8E-09	5.26	31.1
M-7	14.2	7.12	136.3	5.0E-09	8.9	41.7

CHAPTER 2

MATERIALS AND METHODS

MATERIALS

Activated Carbons

The activated carbons employed were Superdarco (designated as SD, NORIT[®]) and Ultracarb (designated as UC). SD is wood-based GAC while UC is a bituminous GAC. SD has higher pore volume than UC. Specifically, SD has 0.2 mL/g of micropore (<20 Å) and 0.3 mL/g of mesopore (20–500 Å), while UC has 0.3 mL/g of micropore and 0.1 mL/g of mesopore.

Water Source

Synthetic arsenic containing water was prepared for small-scale column tests with DI water, in which 0.3 mM NaHCO₃, 0.01 M NaCl, 300–2,000 µg/L arsenate, and 0–2,000 µg/L perchlorate were respectively added. Using 0.1 M of NaOH or HCl, the pH of the synthetic water was kept at 6.5±0.2.

To discern arsenic removal performance of developed media in natural groundwater, column tests were **also** conducted using Rutland water, for which the water quality characteristics were as presented in [Table 1.2](#). The arsenic concentration of this water, determined by HVG-AAS was 60.5 µg/L (refer to Report 3163 for further discussion).

Chemicals

Fe(NO₃)₃·9H₂O (Sigma[®]) was used as an iron precursor. Sodium arsenate (Na₂HAsO₄·7H₂O, Sigma[®]) or sodium arsenite (NaAsO₂, As 1,000 mg L⁻¹, Fluka[®]) solution were used without any modification to prepare the arsenate or arsenite stock solutions.

ANALYTICAL PROTOCOLS

Arsenic Analysis

Arsenic concentrations for the work herein were determined with a Shimadzu Atomic Absorption spectrophotometer (AA-6601F) unit with flame atomization that was connected to a hydride generation system (HVG-1, Shimadzu[®]). For this analytical system, the spectrophotometer wavelength was 193.7 nm, the slit width was 1.0 nm, and the lamp current was 12 mA. The 5M HCl and reducing agent (5% ascorbic acid and 10% KI, w/v) were blended with the arsenic samples so as to reduce the arsenate to arsenite. The mixed solutions were equilibrated for more than 30 min. The arsenic samples were diluted if this was needed to remain within the standard line of 0–50 µg/L. To determine arsenic concentrations for samples having higher arsenic concentrations (>300 µg/L) and different oxidation As species (arsenite and arsenate), a colorimetric method was conducted which was adapted from Johnson (1971).

Iron Analysis

To test the iron loading amount on tailored GAC, about 0.1–0.2 g of GAC was ashed at 600°C and then acid digested with 25 mL of concentrated HCl. The digestion solutions were analyzed for iron by a Shimadzu Atomic Absorption spectrophotometer (AA-6601F) unit with flame atomization.

X-ray Diffraction Analysis

X-ray diffraction (XRD) patterns were obtained using Philips X'Pert MPD system, which was equipped with CuK α radiation (40 kV, 30 mA) with a 0.02° step size and 2.5 second step time over the range $10^\circ < 2\theta < 70^\circ$.

METHODS

Rapid Small-scale Column Tests

Mini-columns employed a 1-mL syringe (diameter: 6-mm, length: 10-cm). The empty bed contact times (EBCTs) were 0.8–2 min. Although various range of EBCTs were used, 1 min of EBCT was mainly used for the media of US mesh #100×140 (148–105 μm ; median 126 μm) and US mesh #80×140 (178–105 μm ; median 141 μm). In accordance with the proportional diffusivity similitude (Parette and Cannon 2005), the mini-column tests with 1 min EBCT (100×140 mesh) simulated an EBCT of 8.4 minutes for US mesh #12×40 (1700–425 μm ; median 1060 μm) full-scale media, or 3.5 minutes for US mesh #20×50 (850–300 μm ; median 440 μm). By using this 1-mL syringe mini-column, we could find accurate bulk densities of different media and exclude spent solids from contact with oxygen before future spectroscopic observations.

Arsenic (V) and Arsenic (III) Adsorption as a Function of pH

As (V) and As (III) adsorption experiments were conducted over a range of pH. These tests consistently employed 0.1 g/L media, and an arsenic concentration of 3 mg/L. Sodium arsenate ($\text{Na}_2\text{HAsO}_4 \cdot 7\text{H}_2\text{O}$) or sodium arsenite (NaAsO_2) standards of 1,000 mg/L as arsenic were used to prepare the arsenate or arsenite stock solutions. Deionized distilled water of a predetermined volume was poured into a 1-L volumetric flask. A small volume of arsenic stock solution was added to achieve the target arsenic concentration, then the given mass of adsorbent media was added. Then, the suspension was distributed quickly into several 125-mL polyethylene bottles. The pH was adjusted to prescribed value between 3–11 for each sample using small volumes of acid (HNO_3 , 0.1 M) or base (NaOH , 0.1 M) stock solutions. All samples were mixed in a rotary shaker at 150 rpm and $20 \pm 0.5^\circ\text{C}$. After 8 hrs of shaking, the pH of the samples was readjusted to the target pH conditions. All samples were then shaken again in the rotary shaker for 24 hr, and then the remaining aqueous phase arsenic was monitored.

Preparation of Fe-GAC through Incipient Wetness Impregnation

The authors herein prepared HFO-incorporated-GAC by using the incipient wetness impregnation method that is depicted in [Figure 2.1](#). Iron nitrate nonahydrate $[\text{Fe}(\text{NO}_3)_3 \cdot 9\text{H}_2\text{O}]$, was incorporated as a precursor of iron oxide into the pores of granular-size porous GAC. This study employed various grain sizes of Superdarco, which is a thermally-tailored lignite (refer to Rangel-Mendez et al., 2005 and Nowack et al. 2004), or Ultracarb, which is a commercial bituminous carbon by Siemens Water Technologies. The following tailoring procedure was developed to achieve this impregnation as homogeneously as possible: (1) dissolve the iron precursor in deionized water at given concentrations to have the final volume of an iron-dissolved solution of 1.0–1.5 mL, (2) disperse the iron precursor solution using a 1-mL micropipette over the dried GAC (1 g), (3) dry the solids at room temperature under the hood for one day, and (4) put in a rotary evaporator for Fe oxide/hydroxide precipitation of iron nitrate at a temperature selected from the range of 60–90 °C for 4–12 h. After Fe oxide/hydroxide precipitation, the solids were cooled to room temperature, and then washed with more than 100 bed volumes of deionized water. The washed solids were dried again under the hood for 24 h prior to use. Parenthetically, the authors noticed that after washing the media, the nitrate did not subsequently leach off when the media was used in water treatment service.

Via this protocol, the authors developed several iron-loaded GACs. We varied in precipitation temperature (50–90°C), carbon type (UC or SD), mesh size (80×140, 100×140, or 200×400), and iron loading (3.6–14.2%). Subsequent testing also revealed that these protocols also varied in the nature of the iron that was created (see below). These iron-loaded GAC variants have been listed as M-1 to M-15 in [Table 2.1](#). M-3 and M-6 were prepared with different sizes of Superdarco. Before the incipient wetness impregnation, citrate acid (designated as CA) was added in ferric nitrate solution with 2 mol % (percentage of molar ratio between citrate and Fe).

[Figure 2.2](#) show the preparation schematic for loading a cationic surfactant on iron loaded GAC. A cationic surfactant [Arquad 2C-75 or cetylpyridinium chloride (CPC)] was loaded through an incipient wetness or recirculation impregnation method after preparing Fe tailored GAC. While employing an incipient wetness impregnation method, M-5 was prepared by post-impregnating a cationic surfactant (designated as CS) such as Arquad 2C-75 (Akzo Nobel Surface Chemistry, IL) into M-4. M-13 was prepared by re-circulating a dilute solution of cetylpyridinium chloride monohydrate (CPC) into M-10 for 2 days. The CPC loading was 180 mg CPC/g of M-10. M-8 [Fe(II)-Fe-SD] was prepared by sequentially impregnating ferrous chloride (FeCl_2 , sigma[®]) for M-4 (Fe-SD).

By use of the same protocol as described previously, the dissolved ferrous solution was used for a second impregnation step for M-4. The medias M-9, 10, 11, and 12 were prepared with different masses of ferric nitrate at 60°C. M-14 (Fe (12.1%)-SD, 200×400 mesh) was prepared at 50°C for 20 h. After the Fe impregnation and drying at 50°C, a solution of sodium hydroxide was prepared with a ratio of 0.8 mL (the volume of NaOH solution) for 1 g of iron tailored GAC, and the concentration of NaOH was equal to 0.94 mole of OH⁻/mole of Fe. Then, the prepared NaOH solution was dispersed over the dried Fe-GAC. Then, media was again dried at 50°C for 20 h. Via this method, we intended to increase the Fe content for GAC and induce a more stable condition for HFO to stick onto the pore structures of the GAC. M-15 (CPC-Fe (7.5%)-UC) was prepared with Ultracarb and a 60°C precipitation temperature. By re-

circulating a dilute solution of CPC, CPC was post-impregnated into Fe-UC for 2 days. The CPC loading was in the range of 110–170 mg CPC/g media.

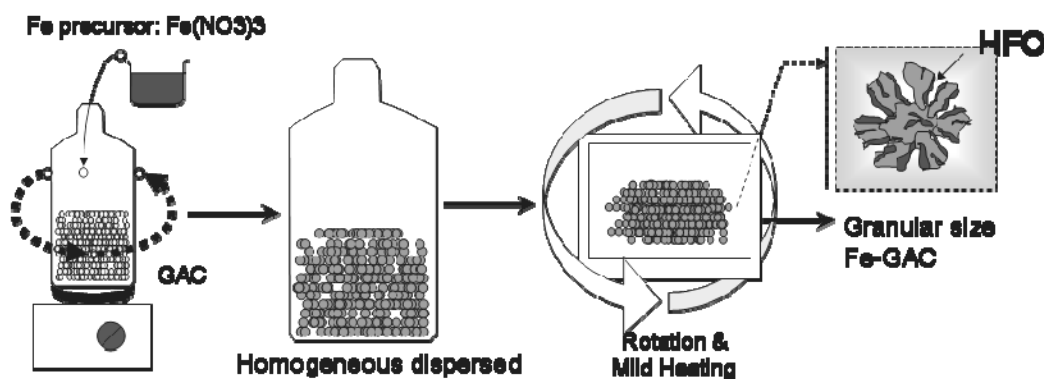


Figure 2.1 Schematic of hydrous ferric oxide impregnated granular activated carbon

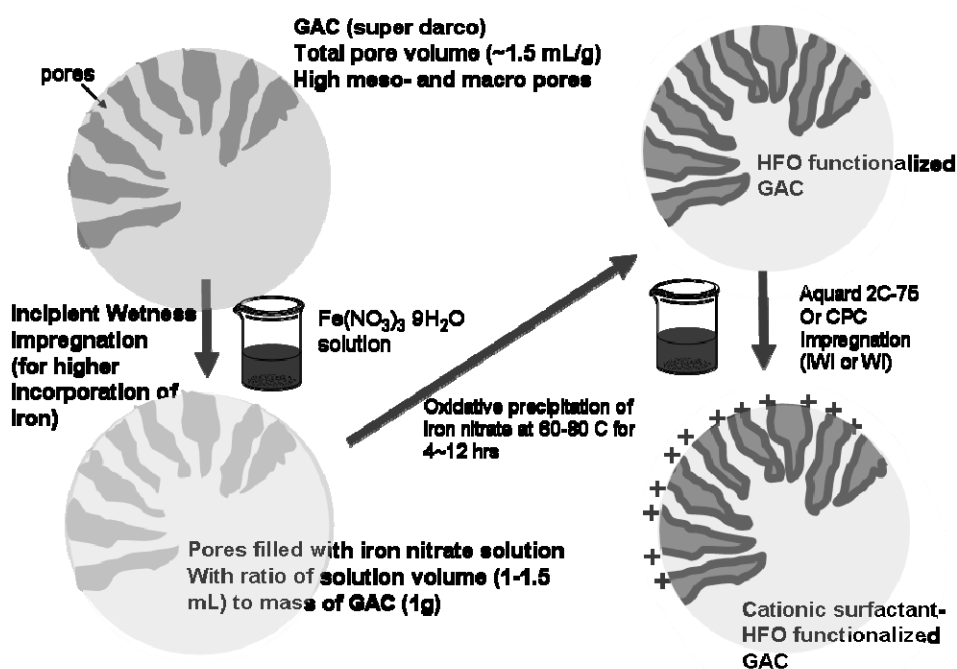


Figure 2.2 Schematics for Fe-GAC and cationic surfactant [Arquard 2C-75 or Cetylpyridinium chloride (CPC)]-Fe-GAC preparation

Table 2.1
Media prepared

ID	Media name	Mesh sizes	Temp. of precipitation [°C] and time [h]	Bulk density [g/mL]	Impregnation percentage of iron [%]	
					Initially prepared	measured
M-1	Fe-UC-200x400-@80*	200×400	80 °C for 6h	0.70	–	3.6
M-2	Fe-SD-200x400-@80†	200×400	80°C for 6h	0.55	–	5.4
M-3	CA-Fe-SD-200x400-@80‡	200×400	80 °C for 6h	0.56	–	6.1
M-4	Fe-SD-80x140-@80	80×140	80 °C for 6h	0.53	20–25	11.0
M-5	CS-Fe-SD-80x140-@80§	80×140	80 °C for 6h	0.52	20–25	10.7
M-6	CA-Fe-SD-80x140-@80	80×140	80 °C for 6h	–	20–25	113
M-7	CA-Fe-SD (1.5mL/g)-80x140-@90**	80×140	90 °C for 4h	0.57	25–30	14.2
M-8	Fe(II)-Fe-SD-80x140-@90††	80×140	90 °C for 4h	0.56	25–35	13.2
M-9	Fe(7.53%)-SD-100x140-@60	100×140	60 °C for 12h	0.35	15	7.5
M-10	Fe(9.2%)-SD-100x140-@60	100×140	60 °C for 12h	0.41	20	9.2
M-11	Fe(10.6%)-SD-100x140-@60	100×140	60 °C for 12h	0.46	25	10.6
M-12	Fe(11.66%)-SD-100x140-@60	100×140	60 °C for 12h	0.51	30	11.7
M-13	CPC-Fe(9.2%)-SD-100x140-@60‡‡	100×140	60 °C for 12h	0.41	20	9.2
M-14	Fe (12.1%)-SD-200x400-@50	200×400	50 °C for 20h	0.55	20	12.1
M-15	CPC-Fe (7.5%)-UC-100x140-@60	100×140	60 °C for 12h	0.60	–	7.5

* Fe impregnated Ultracarb

† Fe impregnated Superdarco

‡ Citrate acid (2 mol %)-assisted iron impregnated Superdarco

§ Cationic surfactant (Arquad 2C-75) post-impregnated Fe-Superdarco

** 1.5 mL/g: iron nitrate solution volume (mL) to GAC mass (g) ratio

†† Fe(II)-Fe-SD: ferrous ions were sequentially impregnated into Fe-Superdarco, FeCl₂ was used as a precursor of ferrous

‡‡ CPC-Fe (9.2%)-SD: cetylpyridinium chloride monohydrate (CPC), loading method: re-circulation wet impregnation, and loading (180 mg CPC/g of M-10)

CHAPTER 3

RESULTS AND DISCUSSION

EFFECT OF PREPARATION TEMPERATURE ON IRON TAILORED GAC

In follow-up to the Contract 3013 work (see Chapter 1), the authors sought to extend the bed life for sorbing arsenic. We recognized from the literature (see Chapter 1) that hydrous ferric oxide (HFO) was the form of iron that offered the highest surface area and highest unit arsenic sorption. So our experiments focused on how to best load HFO into GAC. Within GAC, we reasoned, the fragile HFO could rely on the skeletal strength of the GAC to maintain its physical integrity and character under hydraulic pressures. The previous work lead us to anticipate that HFO favorably formed at lower temperatures than the 80–90°C that we previously appraised; and thus our trials employed a 50–60°C drying temperature for Fe precipitation for the work herein.

Mini-Column Results

Figure 3.1 shows the comparison of column results for media that were prepared at an array of temperatures. These mini-column tests employed the synthetic water that contained 300 µg/L As. The media M-4 was prepared at 80°C for 6 h, while M-9, 10, 11, and 12 were prepared at 60°C for 12 h. As shown in Table 2.1, M-9 to M-12 had 7.5–11.7% of iron loadings.

The column bed lives clearly show that when the media was prepared at 60°C, the Fe (7.53%)-SD (M-9) could remove arsenic for longer bed volumes than the 80°C-prepared media Fe-SD (M-4, Fe 11%). M-9 had about 3,400 BVs to breakthroughs of 50 µg/L, while M-4 broke through to 50 µg/L at 1,500 BVs. Another media prepared at 60°C that gained 9.2% iron (M-10) showed the same breakthrough BVs as M-9, but arsenic concentrations were not detected in the initial period of column operation, as they had been for the M-9 media. Thus, M-10 could give us more reliable arsenic removal. As an interesting aspect, M-9 and M-10 showed slow increases of arsenic concentrations while M-4 showed a sharp increase. This sharp increase phenomenon happened for the media prepared at 90°C (M-8, Fe 13.2%) (Figure 1.5). We propose that these results might be partly due to the formation of more crystallized iron oxide at 80°C or 90°C than at 60°C (see x-ray characterizations below). With crystalline material, the surface is more approachable by As; and thus all sites can be occupied at a concurrent time. This compares to HFO-type iron, where some surface sites are remotely recessed in iron-sided pores, where diffusion rate becomes important.

Other media prepared at 60°C, to 10.6–11.7% Fe loading (M-11 and M-12) showed further increases to 5,300 BVs at 50 µg/L breakthrough when compared with other media. Figure 3.2 shows the comparison of arsenic removal performances according to iron loadings of each media: treated BVs at 50 µg/L of breakthrough and arsenate adsorption capacities based on media and Fe masses. At similar Fe loadings (10–12%), media treated at 60°C had about 3–4 times higher arsenic adsorption capacities than did media treated at 80 or 90°C, based on media or iron mass.

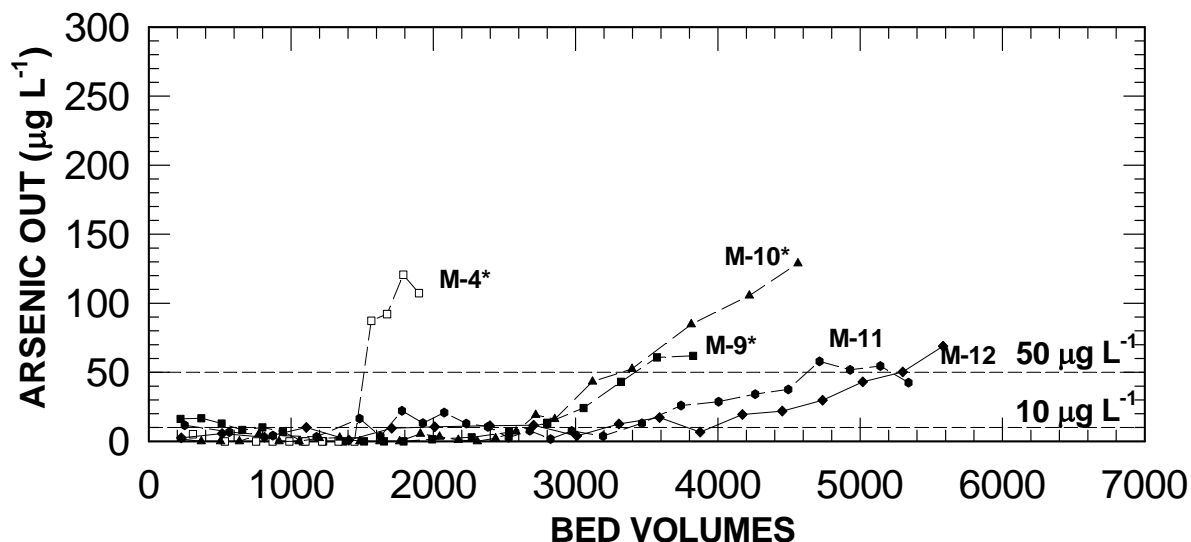


Figure 3.1 Column results of media: M-4 (media loading: 0.4g, EBCT: 1.07 ± 0.04 min, BVs: 0.77 mL), M-9 (media loading: 0.26 g, EBCT: 1.09 ± 0.05 min, BVs: 0.75 mL), M-10 (media loading: 0.3 g, EBCT: 1.09 ± 0.04 min, BVs: 0.73 mL), M-11 (media loading: 0.336 g, EBCT: 1.04 ± 0.1 min, BVs: 0.72 mL), M-12 (media loading: 0.375 g, EBCT: 1 min, BVs: 0.73 mL). Influent As (V) $300 \mu\text{g/L}$, HCO_3^- 0.3 mM, and pH 6.5. M-4, 9, and 10 (Jang et al. 2006b)

Arsenic (V) and Arsenic (III) Adsorption as a Function of pH

The authors characterized As(V) and As(III) adsorption as a function of pH, and these results have been presented in Figure 3.3. These experiments appraised the behavior of two media: the M-4 media that was prepared at 80°C , and the M-9 media that was prepared at 60°C . For the media prepared at 60°C , the arsenate sorption was the same as the arsenite sorption at a pH of 7.5. In contrast, for the media prepared at 80°C , the arsenate removal far exceeded the arsenite removals. It has been reported that HFO can remove arsenite with the same efficiency as arsenate at the crossover pH of 7.5–8.5 (Dixit and Hering 2003), while at pH's below this cross-over point, HFO removes more As(V), and above this pH, HFO removes more As(III). In contrast, more crystalline iron oxides remove more As(V) than As(III) across the pH range. Thus, this result corroborated the x-ray diffraction data (see below), and inferred that the iron oxide that formed in the 60°C media was amorphous HFO, whereas the iron oxide formed in the 80°C media was more crystallized.

Moreover, the media prepared at 60°C with 7.53% Fe showed higher adsorption capacities of both arsenite and arsenate than did the media prepared at 80°C , even though this 80°C media had 11% Fe. At the crossover pH of 7.5 for the 60°C media, both the As(V) and As(III) sorption densities were 130 mg of As/g Fe; and this is as high a sorption density as has been reported for HFO flocs that are stirred in water (see literature above).

Thus, both the sorption-versus-pH tests and the column results showed obvious differences between the media prepared at 60°C versus 80 – 90°C . The main reason for the high adsorption capacity of HFO is that the specific surface area (350 – $600 \text{ m}^2/\text{g}$) of HFO that is

reported in the literature is much greater than those of other crystallized iron oxides such as goethite or magnetite ($<150 \text{ m}^2/\text{g}$).

X-ray diffraction (XRD) analysis

As a further appraisal of whether the 60°C drying had achieved an HFO-type loading, the authors conducted X-ray diffraction analyses with GAC (Superdarco) that had not been preloaded with iron; as compared to iron-tailored GACs that had been loaded with iron and then thermally conditioned at either 60°C, 80°C, or 90°C. Non-preloaded GAC exhibited many crystallized peaks (quartz, [Figure 3.4 \(A\)](#)), indicating that this GAC contained some SiO_2 , as is consistent with coal-based activated carbons that have been acid washed. For the iron impregnated GACs, broad diffraction peaks were shown at 35.9° even though we could not clearly identify relatively smaller peaks at 62.4°. In other references, two-line ferrihydrite (or HFO) shows two broad diffraction peaks at 35.9° and 61.4°, corresponding to d spacings of 0.250 and 0.148 nm, respectively (Van der Giessen 1966, Hofmann et al. 2004). The authors herein note that the peaks observed for the media herein were probably smaller than would be observed in pure iron oxide/hydroxide media, because the iron herein was sorbed inside the GAC pore structure, where the carbon and its ash would mask the signal. None-the-less, a broad shape of peak and position (at 35.9°) seems to indicate that the dominant phase of iron oxide in the 60°C media was HFO. The distinctions in the peak shapes for the various media indicate that these iron oxides exhibited various degrees of crystallinities. Specifically, M-8 prepared at 90 °C exhibited a sharper peak at 35.0° than did the other media. This indicated that the M-8 media contained a higher degree of crystallized iron oxide. The identification of peaks for M-8 corresponded to a dominant phase of akaganéite. For the case of M-4 which was prepared at 80°C, the broad peak of HFO at 35.9° was submerged; and the quartz peaks became relatively diminished, indicating the dominant phase of iron oxide might not be HFO. Presumably, another phase of iron mineral such as Fe_2SiO_4 was manifesting itself.

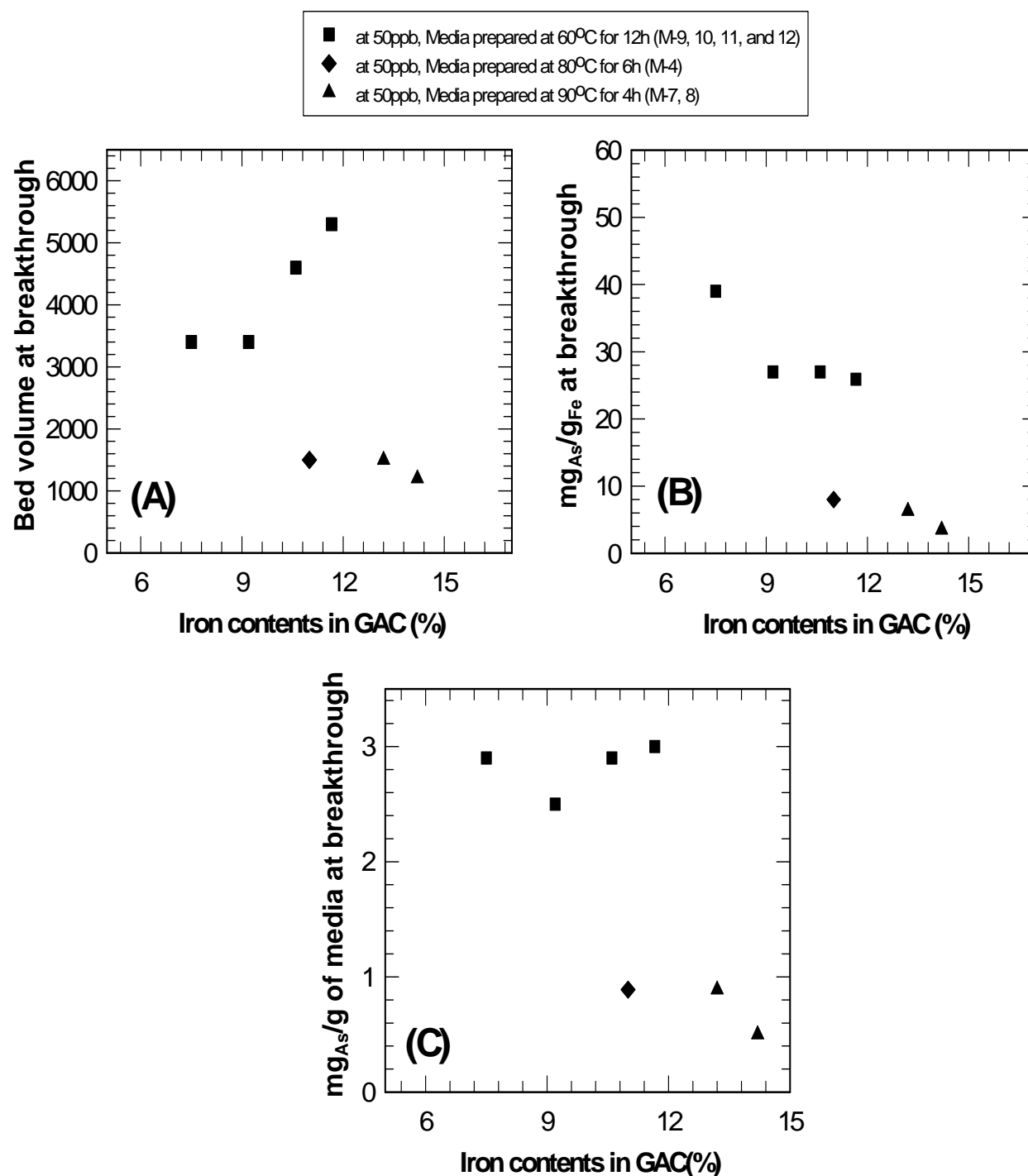


Figure 3.2 Comparisons of arsenic removal performances based on iron loadings for media (A) treated bed volumes at 50 $\mu\text{g/L}$ breakthrough, (B) arsenate adsorption capacities based on Fe content, (C) arsenate adsorption capacities at 50 $\mu\text{g/L}$ breakthrough based on Fe content. For synthetic water with 300 $\mu\text{g/L}$ As.

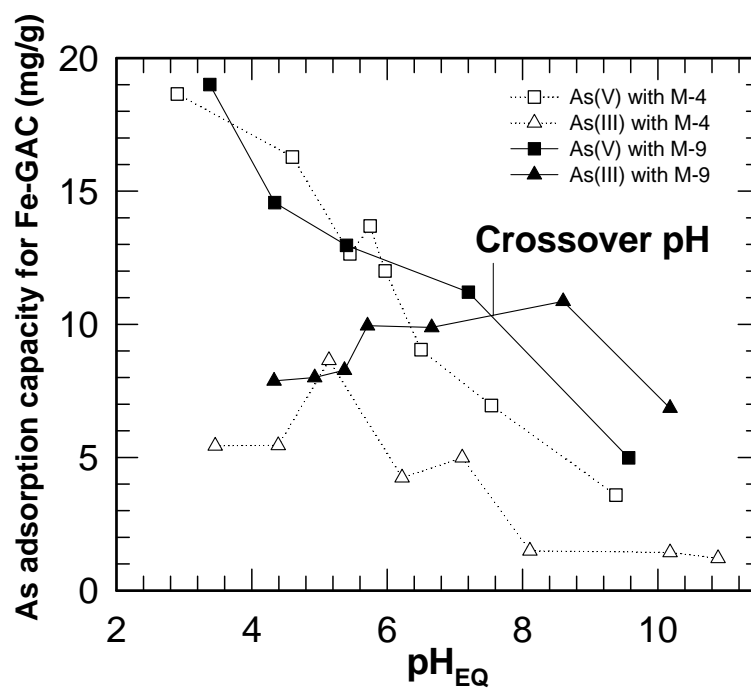


Figure 3.3 Adsorption edge tests of arsenite and arsenate removal for M-4 (Δ/\square , 11%, 80°C, 6h) (Jang et al. 2006b) and M-9 ($\blacktriangle/\blacksquare$, Fe 7.5%, 60°C, 12h). GAC media concentration (0.1 g/L), arsenic concentrations (3 mg/L), stirring times (1 day)

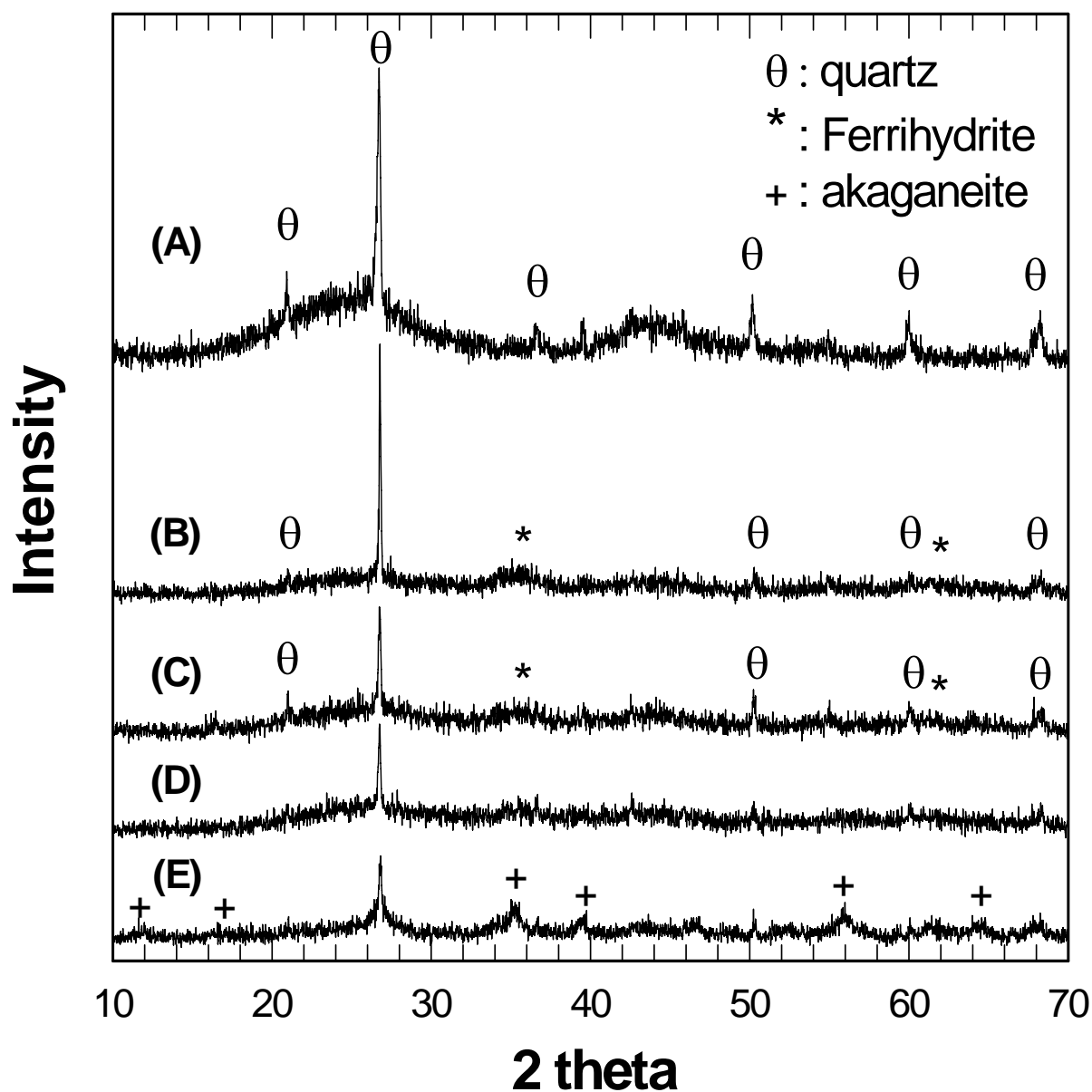


Figure 3.4 XRD results for (A) pure super darco (GAC), (B) M-10 (Fe 9.2%, 60°C, 12h), (C) M-12 (Fe 11.7%, 60°C, 12h), (D) M-4 (Fe 11%, 80°C, 6h), (E) M-8 (Fe 13.2%, 90°C, 4h), θ , +, and * indicate quartz, akaganéite, and 2-line ferrihydrite (or HFO) peaks, respectively.

CATIONIC SURFACTANT LOADED ONTO FE-LOADED GAC

Column Results

The authors immobilized the cationic surfactant cetylpyridinium chloride monohydrate, (CPC) into a media that contained this HFO with 60°C precipitation (M-10, Fe 9.2%). As an ingredient of mouth wash, CPC is a non-toxic chemical (Parette and Cannon 2005). In this test, CPC was post-impregnated using the re-circulation impregnation method, and the media was then washed with 0.001 M NaCl solution. The CPC loading was 180 mg CPC/g of Fe-SD (i.e. 18%), as measured by a mass balance calculation of the CPC.

Figure 3.5 (A) shows the column results of these media. Compared to M-10, the CPC post-impregnated Fe-GAC (M-13) exhibited a 25 or 35% increase in bed volumes to 50 µg/L breakthrough, even though the column using M-13 processed water that contained both 300 µg/L As plus 800 µg/L ClO₄⁻. In contrast, the media that excluded CPC (M-10) processed water that contained only 300 µg/L As. The M-13 offered 34 mg As/g Fe of arsenic adsorption density; and that was 4.3 times higher in value than those of M-4. Figure 3.5 (B) shows the perchlorate removal performance of the column using the M-13 media that employed CPC. No perchlorate was detected till 1,750 BVs; and the bed was saturated with perchlorate at about 3,000 BVs. This media's effectiveness for perchlorate removal was 4.2 mg perchlorate/g of media or 23.5 mg perchlorate/g of CPC. Thus, it can be suggested that the post impregnation of cationic surfactant could not only enhance the arsenic removal performance of iron tailored GAC through making more a positively-charged pathway for the arsenate anion, but it also simultaneously removed perchlorate effectively. This means that this media that contains both iron and cationic surfactant could remediate groundwater that contains both arsenic and perchlorate.

Figure 3.6 shows effluent arsenate concentrations when employing M-15 (CPC-Fe(7.5%)-UC) which was prepared with Ultracarb and dried at 60°C. This media offered 11,000 BVs to 50 µg/L breakthrough. Considering the 7.5% Fe content of this media, these results point to a higher iron efficiency than for previous column results that were obtained with Superdarcobased iron tailored media. Further studies are ongoing to discern the relationship between the structural property of Fe-GAC and arsenic removal performance.

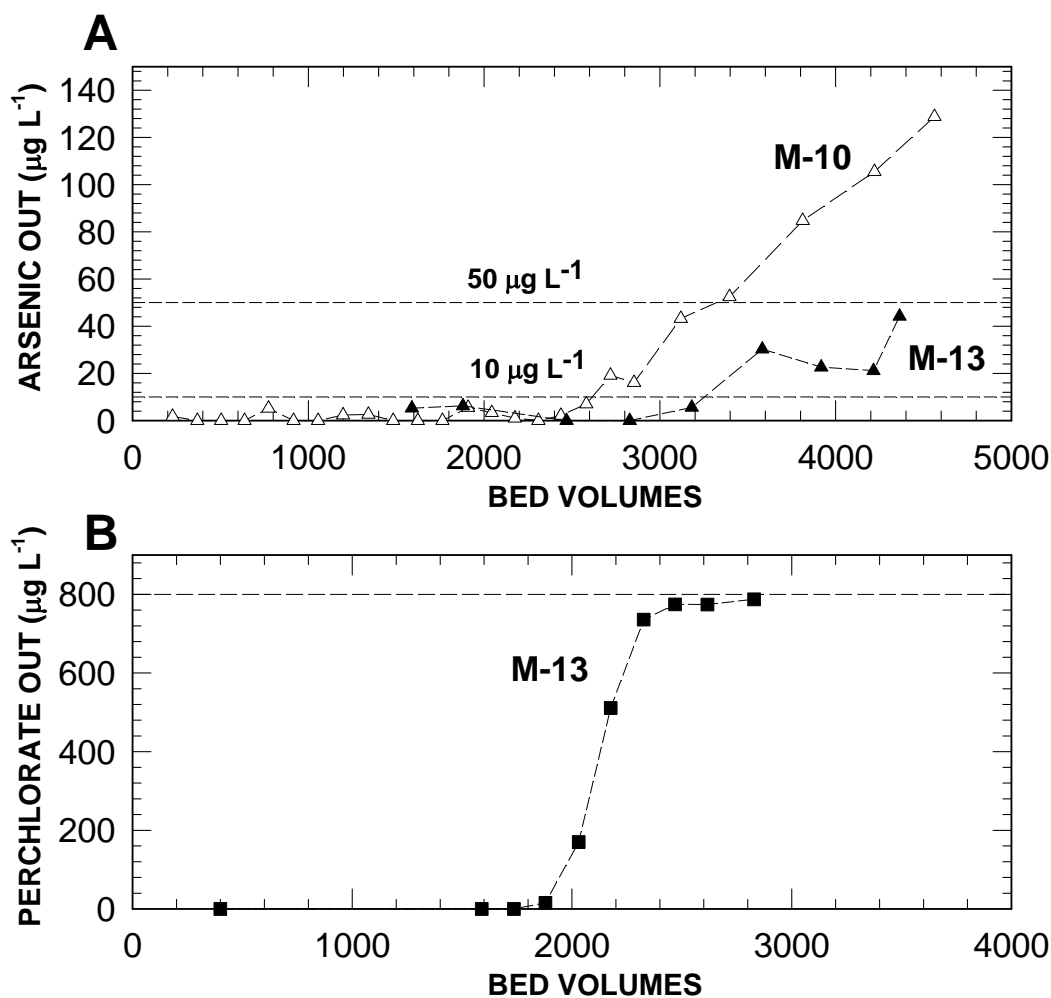


Figure 3.5 Column results: (A) M-10 (Δ), Fe 9.2%, influent arsenate (300 $\mu\text{g/L}$), M-13 (\blacktriangle), Fe 9.2%, (B) perchlorate removal of M-13. All column studies were conducted with the condition: influent arsenate (300 $\mu\text{g/L}$) and perchlorate (800 $\mu\text{g/L}$): both influents contained HCO_3^- 0.3 mM, and pH 6.5, EBCT 1 min

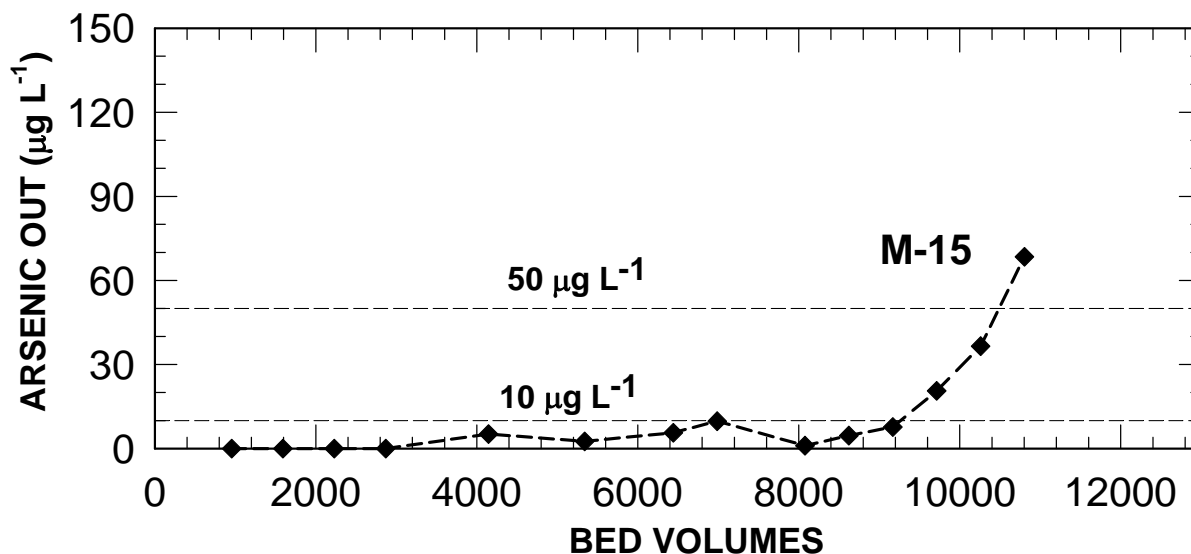


Figure 3.6 Column results of M-15. The column study was conducted with influent arsenate ($300 \mu\text{g/L}$) and perchlorate ($800 \mu\text{g/L}$). Both influents contained 0.3 mM HCO_3^- , and pH 6.5, EBCT 1 min.

Column tests using Rutland water

All of the experiments discussed above have used synthetic water that contained $300 \mu\text{g/L}$ or higher levels of arsenic. This was done to accelerate the bed volumes to break through, so that more media could be tested in less time. However, the authors also sought to determine the performance of several media when processing groundwater from Rutland, MA, which contains $50\text{--}60 \mu\text{g/L}$ As. Specifically, we wanted to appraise how the iron-loaded GAC's developed herein would compare to others reported elsewhere by our Penn State team (Foundation project 3163). For column tests, two different media (100×140 mesh), M-12 and CPC post-impregnated M-12, were used in RSSCT's. In order to discern the performance of perchlorate removal along with arsenic, perchlorate was also added with $40 \mu\text{g/L}$ in the Rutland water. The unadjusted pH remained at $7.6\text{--}8.0$ in, but dropped to $6.5\text{--}7.0$ out, as the media had a mild acidic effect. The EBCT applied was 2 min for these small grains; and this would correspond to a 7 minute EBCT for US mesh $\#20\times 50$ media as per proportional diffusivity similitude.

Figure 3.7 shows the column results of both media. Most data for the M-12 that excluded CPC was less than the detection limit ($0.5 \mu\text{g/L}$) until 12,000 BVs, while some data of CPC post-impregnated M-12 were higher than the detection limit, but less than $10 \mu\text{g/L}$ at $<12,000$ BVs. At around 12,000 BVs, both media exhibited a sharp increase of arsenic concentrations. This result shows that CPC did not help to enhance arsenic removal of Fe-GAC for this case. It is noted that the Rutland water arsenic is about $1/3$ As(III) and $2/3$ As(V); and the As(III) would

carry no charge at neutral pH. Also, there could have been an effect related to competing anions such as sulfate or silicate that the Rutlands water contained but the synthetic water did not. These competing anions could have associated with the pyridinium so as to neutralize its charge when using Rutland water. This affect will be evaluated with further study.

Perchlorate removal performance for both media appears in Figure 3.8. The CPC post-impregnated Fe-GAC treated about 4,300 BVs to breakthrough, while Fe-GAC did not remove perchlorate.

The effect of sodium hydroxide treatment is discerned from the Figure 3.9 data. For this, which column tests employed M-14 (Fe 12.1%) that was precipitated at 50°C followed by the alkaline treatment using sodium hydroxide. For this test, we did not spike perchlorate into Rutland water. We did not adjust the pH, and it remained neutral in the effluent. The breakthrough to 10 µg/L was 16,000 BVs. This result was better than results of Figure 3.7 and Figure 1.4 above.

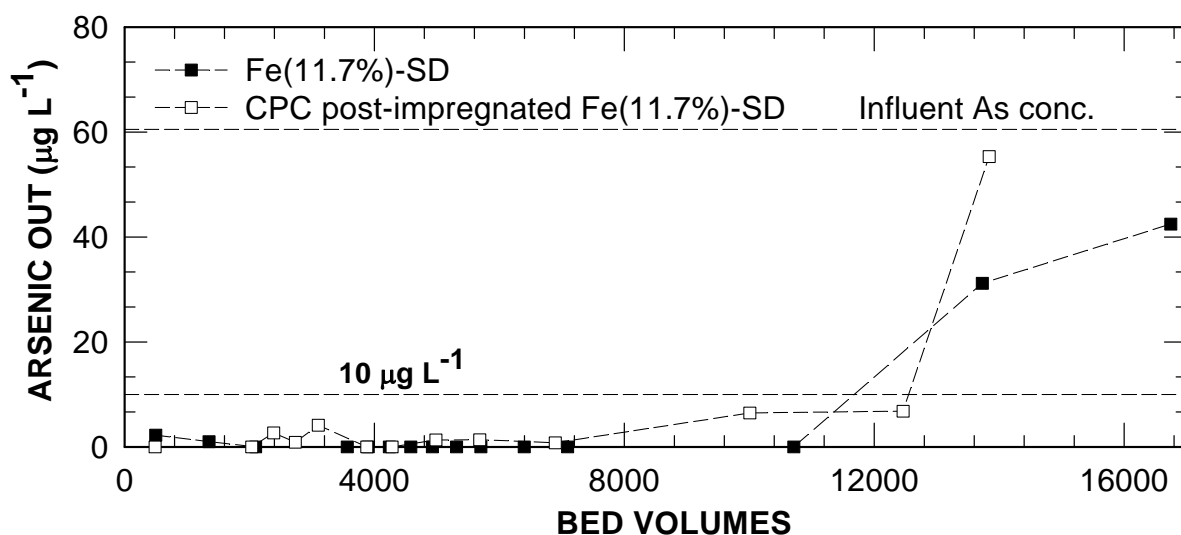


Figure 3.7 Arsenic results of column tests using Rutland water for media (M-12: Fe 11.7%) and CPC post-impregnated Fe (11.7%)-SD (influent arsenic concentrations: 60.5 µg/L and spiked perchlorate concentration: 40 µg/L, 100×140 mesh sizes, media loading: 0.44 g, EBCT: 2 min)

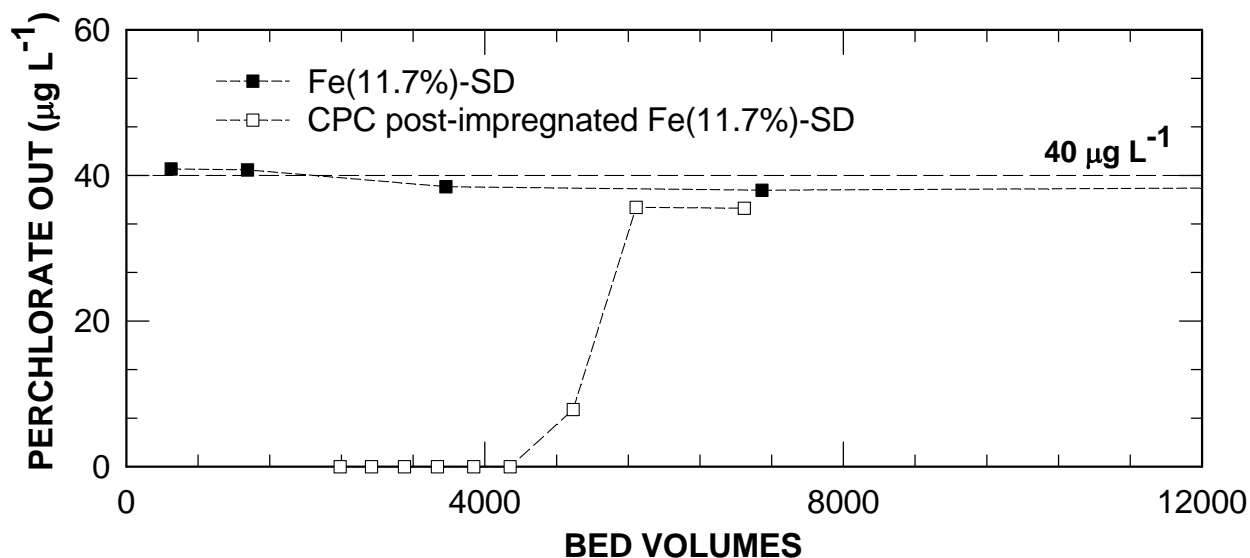


Figure 3.8 Perchlorate results of column tests using Rutland water for media (M-12: Fe 11.7%) and CPC post-impregnated Fe (11.7%)-SD (influent arsenic concentrations: 60.5 µg/L and spiked perchlorate 40 µg/L, 100×140 mesh sizes, media loading: 0.44 g, EBCT: 2 min)

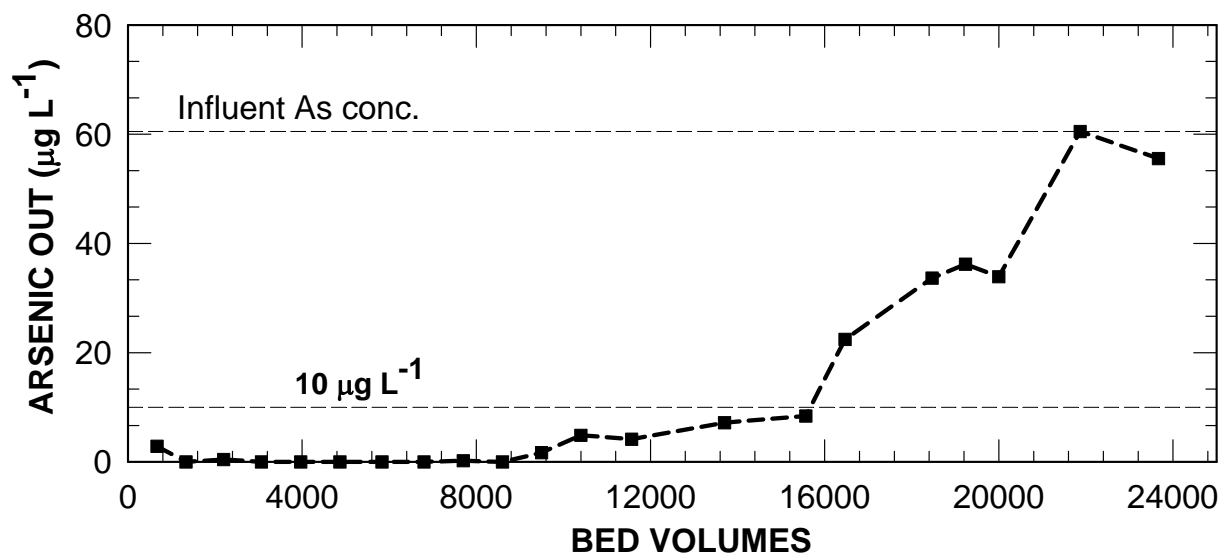


Figure 3.9 Arsenic result of column tests using Rutland water for media (M-14, Fe (12.1%)-SD, arsenic concentration in Rutland water: 60.5 µg/L, 200×400 mesh sizes, loading: 0.84 g, EBCT: 0.75 min)

CHAPTER 4

CONCLUSIONS

The objectives of this study were: (1) to incorporate homogeneously active hydrous ferric oxide into the pores of GAC through an incipient wetness impregnation technique; (2) to evaluate the arsenic adsorption capacities of the media by examining adsorption isotherms, kinetics, and column tests; and (3) to understand the adsorption behavior of the media through physicochemical characterization techniques.

We sought the most favorable temperature for precipitating iron oxide/hydroxide as HFO within GAC, so as to achieve the most favorable arsenic removal performance. At similar Fe loadings (10–12%), the results of column tests showed obvious differences between media prepared at 60°C and 80–90°C: the media treated at 60°C offered about 3–4 times longer bed volumes to As breakthrough than did the media treated at 80–90°C. The arsenic adsorption tests as a function of pH also showed the media treated at 60°C had higher adsorption capacities for both arsenite and arsenate than media prepared at 80°C, even though the Fe content (7.5%) of media prepared at 60°C was much smaller than that (11%) of media prepared at 80°C. For the media prepared at 60°C, there was a pH crossover, at which adsorption capacities of arsenite and arsenate were same. This fact, along with others, indicated that the dominant phase of iron within the GAC was HFO. The main reason for a higher adsorption capacity of HFO is that the specific surface area (350–600 m²/g) of HFO is much greater than those of other crystallized iron oxide such as goethite or magnetite (<150 m²/g). The XRD results of the media treated at 60°C showed the two-line ferrihydrite (or HFO) while the media treated at higher temperatures exhibited a higher degree of crystallinities of iron oxides. The peaks for Fe(II)-Fe-SD (90°C, 4h) indicated dominant phase of akaganéite.

We post-impregnate a cationic surfactant (CPC or Arquad 2C-75) into a Fe tailored GAC. Our hypothesis was that a positively-charged cationic surfactant that lined the mesopores and macropores could streamline the diffusion of arsenate anions through these pores. The column results showed not only about 25–50% of enhancements for arsenic removal, but also high removal performance for perchlorate when using a synthetic solution that contained arsenate.

For the column tests using Rutland water, a media prepared at 80°C with 5.4% iron loading was able to treat about 10,000 BVs before 10 µg/L As breakthrough at pH 6.5. In another column test using Rutland water without adjusting pH, the Fe tailored GAC (Fe 12.1%) treated at 50°C followed by the alkaline treatment had 16,000 BVs of breakthrough to 10 µg/L at neutral pH. Additionally, a cationic surfactant post impregnated HFO-GAC has a high potential in remediating groundwater that contains both arsenic and perchlorate because of its simultaneous removal mechanism.

CHAPTER 5

SIGNIFICANCE TO UTILITIES

As significance to utilities, a new arsenic limit of 10 $\mu\text{g/L}$ became effective in 2006 for the United States drinking water systems. This new regulation would make small public water facilities face heavy financial burdens, unless less costly methods of arsenic removal are developed. There is an urgent demand for an economical, effective, and reliable technique that is capable of removing arsenic species to this new level.

Adsorption onto iron-tailored GAC is considered to be one of the more promising technologies because it is economical and easy to set up, and because the skeletal structure of the GAC is strong, whereas granular iron media are fragile. For the research herein, we focused on devising a synthesis method that would pre-load amorphous hydrous ferric oxide (HFO) into the pores of GAC, so that this active sorptive material could complex both arsenite and arsenate with high sorption capacities. Our aim was to develop a media preparation method that is environmentally acceptable, cost-effective, and simple.

Yet further, our research herein has focused on developing an arsenic removal system that couples the high pore volume, structural cohesiveness, and low costs of granular activated carbon (GAC) with the arsenic-sorbing propensity and low costs of iron. Our overall approach has been to preload iron into the GAC pores in such a manner as to achieve (a) the highest internal loading of iron, while also maintaining (b) the highest efficiency of iron use; i.e. the most mg of arsenic sorbed per gram of iron. When this underlying objective is met, we anticipated, we would achieve the longest bed life for removing arsenic in an easy-to-operate adsorption column, while maintaining low costs. Thus far, we have developed an iron-preloaded media that can remove arsenic to below 10 $\mu\text{g/L}$ for 26,000-33,000 bed volumes; and when this iron tailoring has been coupled with solubilization of zero valent iron in the same vessel, arsenic was removed to below 10 $\mu\text{g/L}$ for 43,000. In prior work, we had observed that when iron solubilization preceded the GAC vessel, we could achieve 150,000 BVs. These tests employed Rutland, MA water, which contained 50-55 $\mu\text{g/L}$ As.

REFERENCES

- Chris, L.X., Yalcin, S., Mingsheng, M., 2000. Speciation of Submicrogram per Liter Levels of Arsenic in Water: On-Site Species Separation Integrated with Sample Collection. *Environ. Sci. Technol.* 34, 2342-2347.
- Chwirka, J.D., Thomson, B.M., Stomp III, J.M., 2000. Removing arsenic from groundwater. *American Water Works Association* 92, 79-88.
- Cumbal, L., Greenleaf, J.E., Leun, D., SenGupta, A.K., 2003. Polymer supported inorganic nanoparticles: characterization and environmental applications. *Reactive & Functional Polymers* 54, 167-180.
- Cumbal, L., SenGupta, A.K., 2005. Arsenic removal using polymer-supported hydrated iron(III) oxide nanoparticles: role of Donnan membrane effect. *Environ. Sci. Technol.* 39, 6508-6515.
- Dixit, S., Hering, J.G., 2003. Comparison of arsenic (V) and arsenic (III) sorption onto iron oxide minerals: implications for arsenic mobility. *Environ. Sci. Technol.* 37, 4182-4189.
- Edwards, M., 1994. Chemistry of arsenic removal during coagulation and Fe-Mn oxidation. *Journal American Water Works Association* 86, 64-78.
- Gilles, G.C., 2000. Advancing arsenic adsorption, specialty media can be used for POU/POE systems. *Water Technology* September.
- Grossl, P.R., Eick, M., Sparks, D.L., Goldberg, S., Ainsworth, C.C., 1997. Arsenate and chromate retention mechanisms on goethite. 2. kinetic evaluation using a pressure-jump relaxation technique. *Environ. Sci. Technol.* 31, 321-326.
- Gu, Z., Fang, J., Deng, B., 2005. Preparation and evaluation of GAC-based iron-containing adsorbents for arsenic removal. *Environ. Sci. Technol.* 39, 3833-3843.
- Haron, M.J., Wan Yunus, W.M.Z., Yong, N.L., Tokunaga, S., 1999. Sorption of Arsenate and Arsenite Anions by Iron(III)-Poly(Hydroxamic Acid) Complex. *Chemosphere* 39, 2459-2466.
- Ho, Y.S., McKay, G., 1998. Kinetic models for the sorption of dye from aqueous solution by wood. *Trans IChemE* 76B, 183-191.
- Hofmann, A., Pelletier, M., Michot, L., Stradner, A., Schurtenberger, P., Kretzschmar, R., 2004. Characterization of the pores in hydrous ferric oxide aggregates formed by freezing and thawing. *J. Colloid. Interf. Sci.* 271, 163-173.
- Ishikawa, T., Nishimori, H., Abe, I., Kandori, K., 1993. Influence of the adsorption of citrate and tartrate ions upon the formation of γ -FeOOH particles. *Colloid. Surface A* 71, 141-146.
- Jackson, B.P., Miller, W.P., 2000. Effectiveness of phosphate and hydroxide for desorption of arsenic and selenium species from iron oxides. *Soil Sci. Soc. Am. J.* 64, 1616-1622.
- Jang, M., F.S. Cannon, R. B. Parette, S.J. Yoon and W.F. Chen. 2009. Combined hydrous ferric oxide and quaternary ammonium surfactant tailoring of granular activated carbon for concurrent arsenate and perchlorate removal; *Water Research*. Vol. 43 (12) pp. 3133-3143.
- Jang, M., Min, S.H., Kim, T.H., Park, J.K., 2006. Removal of arsenite and arsenate using metal oxide incorporated naturally occurring porous diatomite. *Environmental Science and Technology* 40 (5), 1636-1643.
- Jang, M.; W.F. Chen, F.S. Cannon. 2008. Preloading hydrous ferric oxide into granular activated carbon for arsenic removal. *Environmental Science and Technology*. 42, pp. 3369-3374.

- Johnson, D.L., 1971. Simultaneous determination of arsenate and phosphate in natural waters. *Environ. Sci. Technol.* 5, 411-414.
- Johnston, R., Heijnen, H., 2001. *Safe Water Technology for Arsenic Removal*. Dhaka: Bangladesh University of Engineering and Technology.
- Kandori, K., Fukuoka, M., Ishikawa, T., 1991. Effects of citrate ions on the formation of ferric oxide hydroxide particles. *J. Mater. Sci.* 26, 3313-3319.
- Loeppert, R.H., Jain, A., Raven, K.P., Wang, J., 1995. *Arsenate and Arsenite Retention and Release in Oxide and Sulfide Dominated Systems*. College Station, TX: Soil & Crop Sciences Dept., Texas A&M University.
- Mandal, B.K., Chowdhury, T.R., Samanta, G., Basu, G.K., Chowdhury, P.P., Chanda, C.R., Lodh, D., Karan, N.K., Dhar, R.K., Tamili, D.K., Das, D., Saha, K.C., Chakraborti, D., 1996. Arsenic in groundwater in seven districts of West Bengal, India - The biggest arsenic calamity in the world. *Curr Sci India* 70, 976-986.
- Manju, G.N., Raji, C., Anirudhan, T.S., 1998. Evaluation of Coconut Husk Carbon for the Removal of Arsenic From Water. *Water Res.* 32, 3062-3070.
- Manning, B.A., Goldberg, S., 1997. Adsorption and stability of arsenic(III) at the clay mineral-water interface. *Environ. Sci. Technol.* 31, 2005-2011.
- Min, J.H., Hering, J.G., 1998. Arsenate Sorption by Fe(III) Doped Alginate Gels. *Water Res.* 32, 1544-1552.
- Namasivayam, C., Senthilkumar, S., 1998. Removal of Arsenic(V) from Aqueous Solution Using Industrial Solid Waste: Adsorption Rates and Equilibrium Studies. *Ind. Eng. Chem. Res.* 37, 4816-4822.
- Nowack, K.O., F.S. Cannon, D.W. Mazyck. (2004) Enhancing Activated Carbon Adsorption of 2-methylisoborneol: Methane and Steam treatments. *Environmental Science and Technol.* 38, 276-284.
- Pal, B.N., 2001. *Granular Ferric Hydroxide for Elimination of Arsenic from Drinking Water*. Dhaka, Bangladesh. May: Bangladesh University of Engineering and Technology (BUET) and the United Nations University.
- Parette, R., Cannon, F.S., 2005. The removal of perchlorate from groundwater by activated carbon tailored with cationic surfactants. *Water Res.* 39, 4020-4028.
- Parette, R., Cannon, F.S., Weeks, K., 2005. Removing low ppb level perchlorate, RDX, and HMX from groundwater with cetyltrimethylammonium chloride (CTAC) pre-loaded activated carbon. *Water Res.* 39, 4683-4692.
- Rao, M.G., Gupta, A.K., 1982. Ion-exchange processes accompanied by ionic reactions. *Chemical Engineering Journal and the Biochemical Engineering Journal* 24, 181-190.
- Rangel-Mendez, J.R. and F.S. Cannon (2005) Improved activated carbon by thermal treatment in methane and steam: Physicochemical influences on MIB sorption capacity. *Carbon*. 43(3) pp. 467-479.
- Raven, K.P., Jain, A., Loeppert, R.H., 1998. Arsenite and Arsenate Adsorption on Ferrihydrite: Kinetics, Equilibrium, and Adsorption Envelopes. *Environ. Sci. Technol.* 32, 344-349.
- Reddad, Z., Gerente, C., Andres, Y., Le Cloirec, P., 2002. Adsorption of several metal ions onto a low-cost biosorbent: kinetic and equilibrium studies. *Environ. Sci. Technol.* 36, 2067-2073.
- Reed, B.E., Vaughan, R., Jiang, L., 2000. As(III), As(V), Hg, and Pb Removal by Fe-Oxide Impregnated Activated Carbon. *Journal of Environmental Engineering* September, 869-873.

- Scott, M.J., 1991. Kinetics of Adsorption and Redox Processes on Iron and Manganese Oxides: Reactions of As(III) and Se(IV) at Goethite and Birnessite Surfaces. In: Environmental Engineering Science. Pasadena: California Institute of Technology.
- Scott, M.J., Morgan, J.J., 1995. Reactions at Oxide Surfaces. 1. Oxidation of As(III) by Synthetic Birnessite. *Environ. Sci. Technol.* 29, 1898-1905.
- Seki, H., Suzuki, A., 1999. Kinetic study of lead adsorption to composite biopolymer adsorbent. *J Colloid Interf Sci* 211, 375-379.
- Siegel, M., McConnell, P., Ilges, A., Chen, H.-W., Ghassemi, A., Thompson, R., 2006. Development and evaluation of innovative arsenic adsorption technologies for drinking water by the arsenic water technology partnership (SAND2006-0113C). the 2006 NGWA Naturally Occurring Contaminants Conference.
- Smith, A.H., Hopenhayn, R.C., Bates, M.N., Goeden, H.M., Hertz-Picciotto, I., Duggan, H.M., Wood, R., Smith, M.T., Kosnett, M.J., 1992. Cancer Risks from Arsenic in Drinking Water. *Env. Health Persp.* 97, 259-267.
- Sun, X., Doner, H.E., 1998. Adsorption and Oxidation of Arsenite on Goethite. *Soil Science* 163, 278-287.
- Suzuki, T.M., Tanaka, D.A.P., Tanco, M.A.L., Kanesato, M., Yokoyama, T., 2000. Adsorption and Removal of Oxo-Anions of Arsenic and Selenium on the Zirconium(IV) Loaded Polymer Resin Functionalized with Diethylenetriamine-*N,N,N',N'*-Polyacetic Acid. *J. Environ. Monit.* 2, 550-555.
- Thirunavukkarasu, O.S., Viraraghavan, T., Subramanian, K.S., 2003a. Arsenic removal from drinking water using granular ferric hydroxide. *Water SA* 29, 161-170.
- Thirunavukkarasu, O.S., Viraraghavan, T., Subramanian, K.S., 2003b. Arsenic removal from drinking water using iron oxide-coated sand. *Water, Air, and Soil Pollution* 142, 95-111.
- Tokunaga, S., Yokoyama, S.A., Wasay, S.A., 1999. Removal of Arsenic (III) and Arsenic (V) Ions from Aqueous Solutions with Lanthanum (III) Salt and Comparison with Aluminum (III), Calcium (II), and Iron (III) Salts. *Water Environment Research* 71, 299-306.
- Vaishya, R.C., Gupta, S.K., 2003. Arsenic removal from groundwater by iron impregnated sand. *Journal of Environmental Engineering* 129, 89-92.
- Van der Giessen, A.A., 1966. The structure of iron (III) oxide-hydrate gels. *J. Inorg. Nucl. Chem.* 28, 2155-2159.
- Veglio, F., Beolchini, F., Toro, L., 1998. Kinetic modeling of copper biosorption by immobilized biomass. *Industrial & Engineering Chemistry Research* 37, 1107-1111.
- Viraraghavan, T., Subramanian, K.S., Aruldoss, J.A., 1999. Arsenic in drinking water - problems and solutions. *Wat. Sci. Tech.* 40, 69-76.
- Woods, R., 2001. EPA announces arsenic standard for drinking water of 10 parts per billion. Headquarters Press Release, Environmental News.
- Zeng, L., 2003. A method for preparing silica-containing iron (III) oxide adsorbents for arsenic removal. *Water Res.* 37, 4351-4358.

ABBREVIATIONS

AAS	atomic absorption spectrometry
As(III)	arsenite
Arsenate	arsenate
BV	bed volume
C	the concentration of arsenic in the solution
C ⁰	the initial arsenic concentration
CA-Fe-SD	citrate ions added iron incorporated super darco
CPC	cetylpyridinium chloride monohydrate
CS-Fe-SD	cationic surfactant and iron incorporated super darco
CTAC	cetyltrimethylammonium chloride
D _{app}	the apparent diffusivity of arsenic
δ	the liquid film thickness
EBCT	empty bed contact time
Fe(II)-Fe-SD	ferrous ions sequential impregnated iron incorporated surper darco
Fe-GAC	iron incorporated granular activated carbon
Fe-SD	iron incorporated super darco
Fe-UC	iron incorporated ultra carb
GAC	granular activated carbon
HFO	hydrous ferric oxide
HFO-GAC	hydrous ferric oxide incorporated granular activated carbon
HVG	hydride vapor generator
μg/L	microgram per liter
mg/g	miligram per gram
mg/L	miligram per liter
mm	milimeter
POE/POU	point of use/point of entry
ppb	part per billion

R	the average radius of adsorbent particles
RSSCTs	rapid small-scale column tests
SD	super darco
t	time
TDS	total dissolved solid
UC	ultra carb
WHO	world health organization
X	the fraction of the arsenic adsorbed to adsorbent
XRD	X-ray diffraction